

RESEARCH ARTICLE

$\alpha 5$ and αv integrins cooperate to regulate vascular smooth muscle and neural crest functions *in vivo*

Christopher J. Turner*, Kwabena Badu-Nkansah, Denise Crowley, Arjan van der Flier and Richard O. Hynes^{‡,§}**ABSTRACT**

The RGD-binding $\alpha 5$ and αv integrins have been shown to be key regulators of vascular smooth muscle cell (vSMC) function *in vitro*. However, their role on vSMCs during vascular development *in vivo* remains unclear. To address this issue, we have generated mice that lack $\alpha 5$, αv or both $\alpha 5$ and αv integrins on their vSMCs, using the *SM22 α -Cre* transgenic mouse line. To our surprise, neither $\alpha 5$ nor αv mutants displayed any obvious vascular defects during embryonic development. By contrast, mice lacking both $\alpha 5$ and αv integrins developed interrupted aortic arches, large brachiocephalic/carotid artery aneurysms and cardiac septation defects, but developed extensive and apparently normal vasculature in the skin. Cardiovascular defects were also found, along with cleft palates and ectopically located thymi, in *Wnt1-Cre* $\alpha 5/\alpha v$ mutants, suggesting that $\alpha 5$ and αv cooperate on neural crest-derived cells to control the remodelling of the pharyngeal arches and the septation of the heart and outflow tract. Analysis of cultured $\alpha 5/\alpha v$ -deficient vSMCs suggests that this is achieved, at least in part, through proper assembly of RGD-containing extracellular matrix proteins and the correct incorporation and activation of latent TGF- β .

KEY WORDS: Aneurysms, Blood vessels, Cardiovascular development, Integrin, Neural crest, Vascular smooth muscle cells

INTRODUCTION

Vascular smooth muscle cells (vSMCs) are specialised cells found wrapped around arteries, arterioles and large veins. Most vSMCs are derived from the mesoderm (Mikawa and Gourdie, 1996; Wasteson et al., 2008); however, vSMCs surrounding the ascending aorta and aortic arch are derived from the neural crest (Jiang et al., 2000), whereas vSMCs at the aortic root originate from the secondary heart field (Waldo et al., 2005). During development, a major function of vSMCs is to synthesise and assemble large quantities of extracellular matrix (ECM) around newly formed vessels to provide the vasculature with elasticity and structural strength to withstand the pulsatile blood flow from the heart. The ECM deposited around the vasculature has many functions beyond this structural role however (Hynes, 2009). Previous studies have shown that the ECM within the vessel wall regulates the attachment, contractility, motility, proliferation and differentiation of vSMCs (Raines, 2000). Furthermore, it is now clear that the ECM plays an important role in the patterning and development of the vascular

system by binding to, and regulating the availability and activity of, numerous growth factors and morphogens.

The interaction of transforming growth factor β (TGF- β) with the ECM in particular appears essential for regulating cardiovascular morphogenesis and function (ten Dijke and Arthur, 2007; Horiguchi et al., 2012). TGF- β is synthesised as an inactive complex bound to a latent associated protein (LAP) and is incorporated into the ECM through covalently binding to latent TGF- β -binding proteins (specifically LTBP-1, -3 and -4; Ltbp1, 3 and 4, respectively – Mouse Genome Informatics) that interact with fibrillin-containing microfibrils within the vessel wall. This interaction not only localises TGF- β to specific sites but also regulates its activation. Mice lacking the long form of Ltbp1 (Ltbp1L) (Todorovic et al., 2007), just like *Tgfb* KO mice (Molin et al., 2004) and neural crest-specific *Tgfb*2 mutants (Choudhary et al., 2009), die around birth from defects in septation of the heart, cardiac outflow tract and abnormal remodelling of the pharyngeal arch arteries (PAAAs), due to decreased TGF- β signalling (Todorovic et al., 2007).

Interestingly, a recent study has shown that assembly of the glycoprotein fibronectin, rather than fibrillin 1, is essential for incorporation of Ltbp1 into the ECM by vSMCs (Zilberberg et al., 2012). Fibronectin is one of the first ECM proteins to be expressed around the vasculature and is essential for cardiovascular development (Astrof and Hynes, 2009). Fibronectin-null mice die at embryonic day (E) 9.5 with defects in the formation of the heart, dorsal aortae and yolk sac vasculature (George et al., 1993, 1997). Assembly of fibronectin occurs predominantly through the binding of the heterodimeric cell surface adhesion receptor integrin $\alpha 5\beta 1$ to the Arg-Gly-Asp (RGD) motif in fibronectin. In its absence, however, αv integrins ($\alpha v\beta 1$, $\alpha v\beta 3$, $\alpha v\beta 5$, $\alpha v\beta 6$ and $\alpha v\beta 8$), which also recognise the RGD tripeptide, can relocate to focal contacts previously occupied by $\alpha 5\beta 1$ and assemble fibronectin (Yang and Hynes, 1996; Takahashi et al., 2007; van der Flier et al., 2010). The fibronectin fibrils produced by αv integrins, however, appear short and thick, rather than the long, thin dense fibrillar network produced by cells expressing $\alpha 5\beta 1$ (Takahashi et al., 2007; van der Flier et al., 2010).

$\alpha 5$ and αv integrins play key roles in the development of the vasculature (Hynes, 2007). Integrin- $\alpha 5$ KO mice die at E10.5 with severe vascular defects (Yang et al., 1993; Francis et al., 2002; Mittal et al., 2013), whereas genetic ablation of all five αv integrins leads to placental defects and haemorrhaging within the brain (Bader et al., 1998). Endothelium-specific deletion of both $\alpha 5$ and αv subunits, however, fails to replicate the angiogenic defects observed in global KO-mice, but instead leads to defects in the remodelling of the heart and great vessels (van der Flier et al., 2010). Interestingly, despite the requirement for both $\alpha 5$ and αv integrins for assembly of fibronectin *in vitro*, fibronectin fibrils are clearly present within the basement membrane of endothelium-specific $\alpha 5/\alpha v$ mutants (van der Flier et al., 2010), suggesting that fibronectin is assembled by $\alpha 5$ and αv integrins expressed on

Howard Hughes Medical Institute, Koch Institute for Integrative Cancer Research, Massachusetts Institute of Technology, Cambridge, MA 02139, USA.

*Present address: University Campus Suffolk, James Hehir Building, Neptune Quay, Ipswich, IP4 1QJ, UK.

[‡]Present address: Biogen Idec, 14 Cambridge Center, Cambridge, MA 02142, USA.

[§]Author for correspondence (rohynes@mit.edu)

vSMCs, or by other fibronectin-binding integrins present on the endothelium, such as $\alpha4\beta1$ and $\alpha9\beta1$.

In vitro, both $\alpha5$ and αv integrins are essential for regulating the functions of vSMCs (Moiseeva, 2001). Integrin $\alpha5\beta1$ is highly expressed on vSMCs and has been shown to promote proliferation, migration and switching of vSMCs from a more ‘contractile’ to a ‘synthetic’ phenotype (Hedin and Thyberg, 1987; Barillari et al., 2001; Davenpeck et al., 2001; Rensen et al., 2007). Similarly, αv integrins (in particular $\alpha v\beta3$) have been implicated in controlling vSMC migration, de-differentiation, contractility, proliferation and apoptosis (Liaw et al., 1995; D’Angelo et al., 1997; Panda et al., 1997; Dahm and Bowers, 1998). However, the role of $\alpha5$ and αv integrins on vSMCs *in vivo* remains unclear. Deletion of $\alpha5$ using *Pdgfrb-Cre*, which targets both pericytes and vSMCs (Foo et al., 2006), results in embryonic lethality due to lymphatic, rather than vSMC defects (Turner et al., 2014), whereas arteries in the retinas of mice completely deficient in $\alpha v\beta3$ display only minor delays in recruitment and attachment of vSMCs (Scheppke et al., 2012). Therefore, to gain further insight into the functions of both $\alpha5$ and αv integrins *in vivo*, we have generated mice that lack *Itga5* and *Itgav* specifically within their vSMCs.

RESULTS

SM22 α -Cre-mediated deletion of both $\alpha5$ and αv integrins leads to late embryonic lethality

To investigate the role of $\alpha5$ and αv integrins on vSMCs *in vivo*, we crossed female double-homozygous *Itga5/Itgav*-floxed mice to male double-heterozygous *Itga5/Itgav* KO mice carrying the *SM22 α -Cre* recombinase. *SM22 α -Cre* is expressed within differentiated vSMCs throughout the vasculature (supplementary material Fig. S1) (Holtwick et al., 2002; Yang et al., 2010). This generated four informative genotypes: (1) control mice, (2) $\alpha5$ integrin-deficient mutants (hereafter referred to as *Itga5*^{SM22-Cre}), (3) αv integrin-deficient mutants (hereafter *Itgav*^{SM22-Cre}) and (4) $\alpha5/\alpha v$ conditional double-KO mutants (hereafter *Itga5/av*^{SM22-Cre}).

Examination of offspring revealed that both *Itga5*^{SM22-Cre} and *Itgav*^{SM22-Cre} mutants survive embryonic development, but display high rates (~50%) of postnatal lethality (supplementary material Fig. S2). *SM22 α -Cre*-mediated deletion of both $\alpha5$ and αv integrins, however, resulted in embryonic lethality from E16.5, and no living *Itga5/av*^{SM22-Cre} mice were ever obtained after birth (supplementary material Fig. S2). Analysis of late gestation mice revealed development of extensive vasculature and no obvious haemorrhaging or oedema in any of the mutant embryos (supplementary material Fig. S3); however, a small number of *Itga5/av*^{SM22-Cre} mice did appear slightly growth retarded and occasionally pale in colour.

***Itga5/av*^{SM22-Cre} mutant mice display abnormal remodelling of the PAAs and cardiovascular defects**

To determine the cause of lethality in *Itga5/av*^{SM22-Cre} mice, mutant embryos were isolated at E17.5 and imaged using a micro-CT scanner. This revealed that *Itga5/av*^{SM22-Cre} embryos develop severe cardiovascular defects (Fig. 1). In contrast to control, *Itga5*^{SM22-Cre} and *Itgav*^{SM22-Cre} embryos, in which the aorta arises from the left ventricle and arches over the heart and descends posteriorly as the descending aorta (Fig. 1A), in *Itga5/av*^{SM22-Cre} mice, the ascending aorta misses its connection to the descending aorta (Fig. 1B,C). As the missing portion of the aortic arch is between the left carotid and subclavian arteries, this is equivalent to the clinically defined type-B interrupted aortic arch. Micro-CT scans also revealed that E17.5 *Itga5/av*^{SM22-Cre} embryos displayed a large aneurysm at the

brachiocephalic artery and the proximal region of the right carotid artery (Fig. 1B). Interestingly, interrupted aortic arch type-B is also seen in several TGF- β signalling mutants (Molin et al., 2004; Todorovic et al., 2007; Choudhary et al., 2009). Furthermore, neural crest-specific *Tgfr2* mutants (herein referred to as *Tgfr2*^{Wnt1-Cre}) display an interrupted aortic arch and an aneurysm in the brachiocephalic region just as observed in *Itga5/av*^{SM22-Cre} embryos (Choudhary et al., 2009).

In addition to abnormal remodelling of the PAAs, *Itga5/av*^{SM22-Cre} embryos also displayed defects in septation of the outflow tract (conotruncus) and ventricles of the heart (Fig. 1D-G). In wild-type mice, cardiac septation is usually complete between E13.5 and E14.5 (Savolainen et al., 2009) (Fig. 1D). However, by E17.5, *Itga5/av*^{SM22-Cre} mutants had failed to separate the most proximal region of the outflow tract into the aorta and pulmonary artery (Fig. 1E), a defect known as persistent truncus arteriosus (PTA), and were missing the rostral proportion of the ventricular septum (Fig. 1G). Surprisingly, despite these severe defects in development of the heart and aortic arches, no obvious vascular defects were observed in other tissues analysed. Whole-mount immunofluorescence staining of blood vessels within the skin revealed that $\alpha5/\alpha v$ -deficient mesodermal vSMCs appeared indistinguishable from control cells. vSMCs surrounding dermal arteries in *Itga5/av*^{SM22-Cre} embryos appeared aligned, tightly attached and expressed high levels of the contractile protein α -smooth muscle actin (α SMA) (Fig. 1H).

Neural crest-specific ablation of both $\alpha5$ and αv integrins leads to cardiovascular defects

During early embryonic development (at ~E9.5 in mice), cardiac neural crest cells (CNCCs) from the dorsal neural tube migrate along the third, fourth and sixth PAAs and invade the cardiac outflow tract of the heart. Here, they proliferate, condense and form the aorticopulmonary septum, which divides the single-tubed vessel into the ascending aorta and pulmonary trunk (Kirby et al., 1983; Kirby and Waldo, 1995; Jiang et al., 2000). In addition, CNCCs covering the PAAs have a separate role, as they differentiate into vSMCs and help co-ordinate patterning of the aortic arch arteries. The physiological importance of CNCCs in development of the cardiovascular system can be seen in ablation studies carried out in chicken embryos. Loss of CNCCs leads to abnormal remodelling of the aortic arches, defects in the septation of the outflow tract and disrupted formation of the thymus (Kirby and Waldo, 1995).

As vascular defects were observed in *Itga5/av*^{SM22-Cre} embryos only in areas known to be dependent on CNCCs, we crossed female double-homozygous *Itga5/Itgav*-floxed mice to male double-heterozygous *Itga5/Itgav* KO mice carrying the *Wnt1-Cre* recombinase, to test whether the phenotype of *Itga5/av*^{SM22-Cre} embryos was in fact due to defects in neural crest-derived cells. As expected, *Wnt1-Cre* was expressed throughout the neural crest (supplementary material Fig. S4A) and in vSMCs surrounding the ascending aorta, aortic arch and carotid arteries (Fig. 2A).

Consistent with an essential role for $\alpha5$ and αv integrins in neural crest function (Mittal et al., 2010), most *Itga5*^{Wnt1-Cre}, *Itgav*^{Wnt1-Cre} and *Itga5/av*^{Wnt1-Cre} mutants died at around birth (supplementary material Fig. S5). However, only *Itga5/av*^{Wnt1-Cre} mutants displayed cardiovascular defects (Fig. 2B-G). Just as observed in *Itga5/av*^{SM22-Cre} mutants, *Itga5/av*^{Wnt1-Cre} embryos developed PTA (Fig. 2B-E) and ventricular septal defects (Fig. 2F,G), confirming that the phenotype of *Itga5/av*^{SM22-Cre} is largely due to loss of $\alpha5$ and αv integrins on CNCCs. Genetic deletion of both $\alpha5$ and αv integrins did not appear to affect neural crest cell distribution in

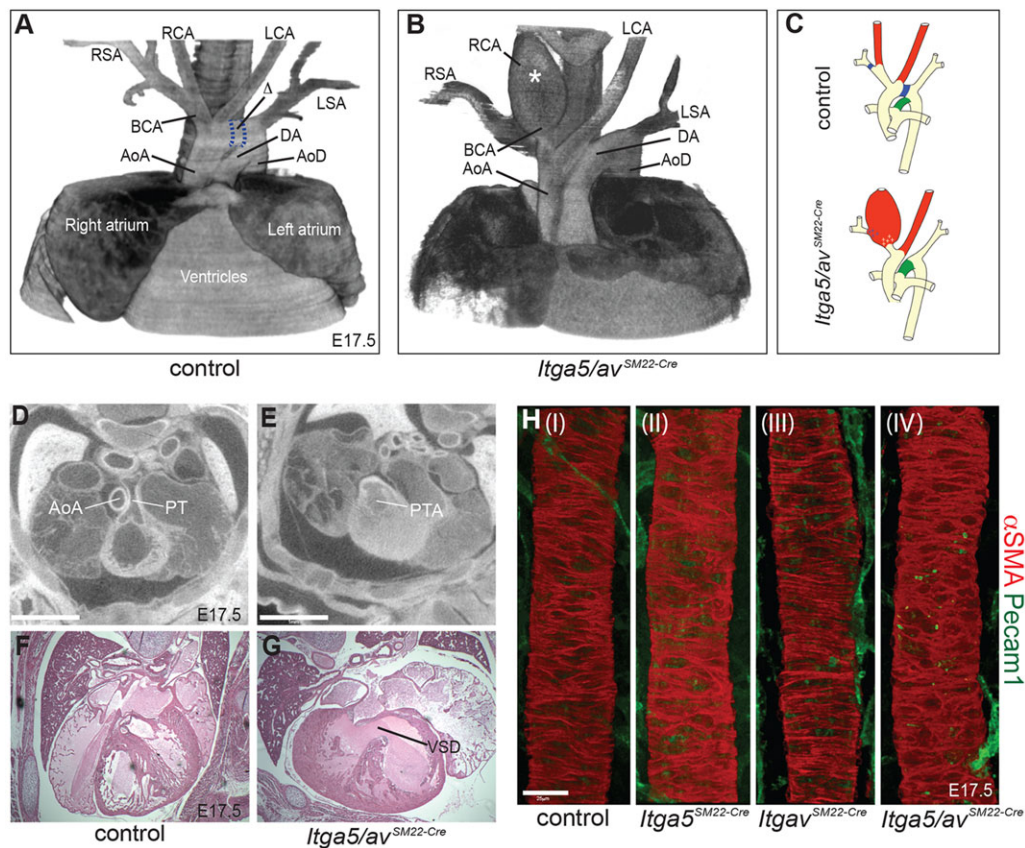


Fig. 1. Cardiovascular defects in *Itga5/av*^{SM22-Cre} mice. (A,B) Three-dimensional (3D)-rendered micro-CT images of the pharyngeal arch arteries in E17.5 embryos. (A) Control and (B) *Itga5/av*^{SM22-Cre} mutant embryos displaying an interrupted aortic arch (type-B) with dilation of the brachiocephalic artery and proximal portion of the carotid artery (indicated by asterisk). The atria have been removed to allow better visualization of the aortic arch. Note that the region of the aortic arch that is derived from the IV pharyngeal arch in the control (Δ , outlined in blue in A, which corresponds with the blue region in C), is missing in the *Itga5/av*^{SM22-Cre} mutant (B). (C) Schematic of the PAAs (III, red; IV, blue; VI, green) in an E17.5 control and *Itga5/av*^{SM22-Cre} mutant [modified from Papangeli and Scambler (2013)]. (D,E) Micro-CT sections showing normal septation of the outflow tract into ascending aorta (AoA) and pulmonary trunk (PT) in a control embryo (D) and PTA in an *Itga5/av*^{SM22-Cre} embryo (E) at E17.5. (F,G) H&E staining of E17.5 heart sections, demonstrating normal cardiac septation in control (F) and ventricular septation defects (VSDs) in *Itga5/av*^{SM22-Cre} embryos (G). (H) Whole-mount immunofluorescence images showing normal association of vSMCs (α SMA, red) around blood vessels (Pecam1, green) within the skin of (I) control, (II) *Itga5*^{SM22-Cre}, (III) *Itgav*^{SM22-Cre} and (IV) *Itga5/av*^{SM22-Cre} mutant embryos at E17.5. RSA/LSA, right/left subclavian artery; RCA/LCA, right/left carotid arteries; BCA, brachiocephalic artery; DA, ductus arteriosus; AoA, ascending aorta; AoD, descending aorta; PAA, pharyngeal arch arteries; PTA, persistent truncus arteriosus. Scale bars: 1 mm in D,E; 25 μ m in H.

early *Itga5/av*^{Wnt1-Cre} mutants however. Analysis of whole-mount X-Gal-stained *Itga5/av*^{Wnt1-Cre} embryos containing the Rosa26 *lacZ* reporter revealed an overtly normal pattern of neural crest cells in mutant mice (supplementary material Fig. S4A–D). Moreover, CNCCs were clearly present in the outflow tracts of E11.5 *Itga5/Itgav*^{Wnt1-Cre} mutants (supplementary material Fig. S4B,D), indicating that loss of both $\alpha 5$ and αv integrins does not compromise CNCC migration. However, in contrast to *Itga5/av*^{SM22-Cre} embryos, *Itga5/av*^{Wnt1-Cre} embryos rarely developed defects in remodelling of the aortic arch (1/6) and never developed the large aneurysms at the brachiocephalic artery (Fig. 2C), suggesting that the remodelling of the PAAs is dependent on both mesodermal and neural crest-derived vSMCs.

***Itga5/Itgav*^{Wnt1-Cre} mice have ectopically located thymi and cleft palates**

In addition to cardiovascular defects, *Itga5/av*^{Wnt1-Cre} mice also displayed defects in the positioning of their thymus. At E17.5, the two lobes of the thymus should be positioned above the heart (Fig. 2H). In *Itga5/av*^{Wnt1-Cre} embryos, however, at least one lobe of the thymus was often ectopically located in the cervical region

(Fig. 2I). Once again, mirroring the defects in *Tgfb2*^{Wnt1-Cre} mutants (Ito et al., 2003), *Itga5/Itgav*^{Wnt1-Cre} mice also developed a cleft palate (Fig. 2J,K). Fusion of palatal shelves is normally complete by E14.5 in control mice. Palatal shelves in *Itga5/Itgav*^{Wnt1-Cre} mice, however, remained small and failed to fuse at the midline by E17.5 (Fig. 2K).

Normal vSMC differentiation in *Itga5/av*^{SM22-Cre} mutants

A crucial step in the formation of the great arteries is the differentiation of CNCCs into highly contractile vSMCs. Neural crest-specific deletion of *Tgfb2* (Wurdak et al., 2005), *Smad2* (Xie et al., 2013), *Notch* (High et al., 2007) or the myocardial-related transcription factor B (Li et al., 2005) all lead to defects in vSMC differentiation and abnormal development of the outflow tract and aortic arch arteries. Failure to differentiate CNCCs into vSMCs was not the cause of the defects in *Itga5/av*^{SM22-Cre} embryos however. Expression of the early vSMC markers α SMA and smooth muscle myosin heavy chain 11 (Myh11) were clearly visible in CNCC-derived cells surrounding the brachiocephalic artery (supplementary material Fig. S6A) and PAAs (data not shown) at E11.5, and continued to be expressed

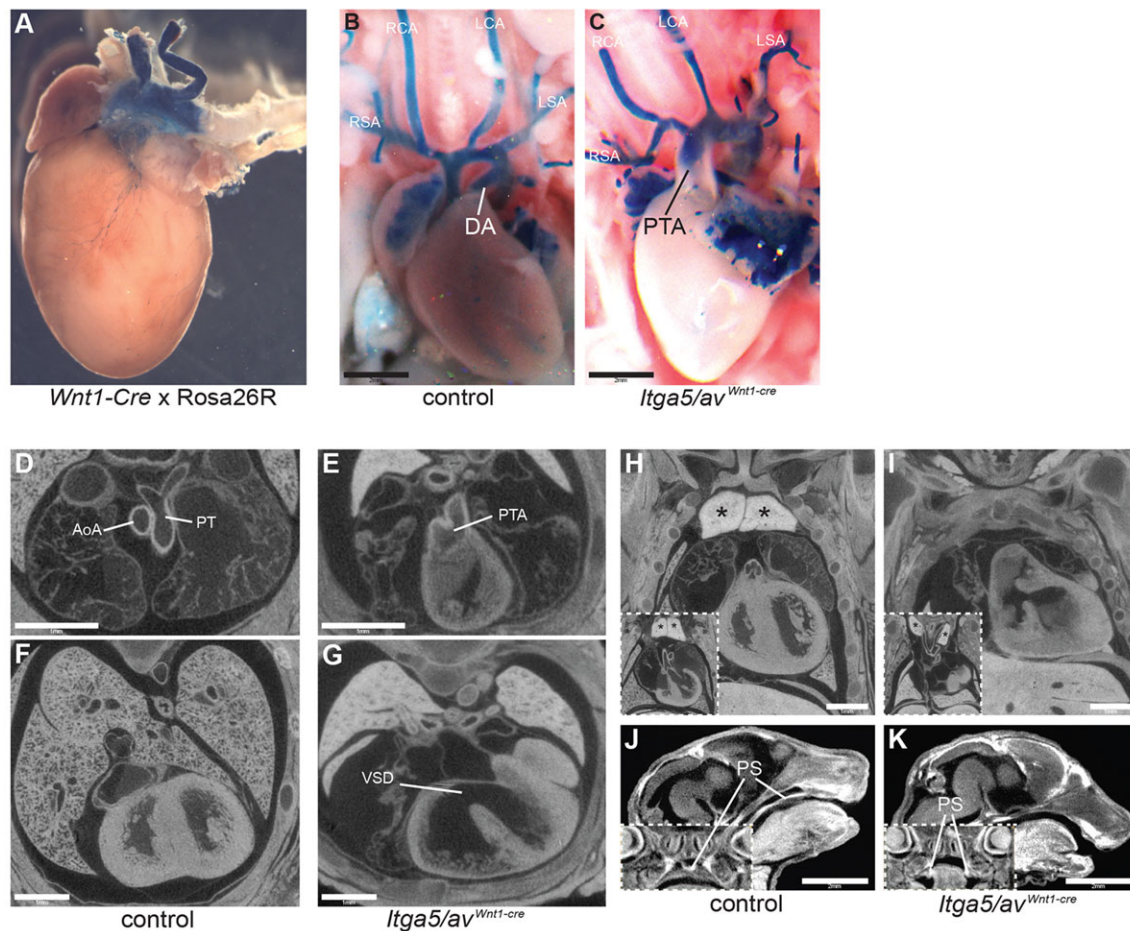


Fig. 2. Integrins $\alpha 5$ and αv are essential for cardiac neural crest function. (A-C) β -gal staining confirming *Wnt1-Cre* expression in neural crest-derived vSMCs surrounding the aortic arch and carotid arteries of an adult mouse. Vascular casts (blue) showing the patterning of the aortic arch arteries in a control (B) and an *Itga5/av^{Wnt1-Cre}* embryo with PTA at E17.5 (C). (D-K) Micro-CT sections through a control and *Itga5/av^{Wnt1-Cre}* embryo at E17.5. Instead of displaying a distinct ascending aorta (AoA) and pulmonary trunk (PT) (see D), the outflow tract of *Itga5/av^{Wnt1-Cre}* embryos remained a single vessel, leading to PTA (see E). Complete ventricular septation in a control (F) and VSD in an *Itga5/av^{Wnt1-Cre}* embryo (G). Correct position of the thymus in a control (H) and ectopic location of both thymic lobes in an *Itga5/av^{Wnt1-Cre}* embryo (I). Normal formation of the palatal shelf (PS) in control (J) and cleft palate in an *Itga5/av^{Wnt1-Cre}* embryo (K). Inserts in H-K show additional frontal views of scans. Scale bars: 2 mm in B,C; 1 mm in D-I; 2 mm in J,K.

around the great vessels until lethality at E17.5 (supplementary material Fig. S6B-D).

Abnormal vSMC morphology in the right carotid artery of *Itga5/av^{SM22-Cre}* mutants

Although the differentiation of vSMCs appeared unaffected by the loss of $\alpha 5$ and αv integrins, immunofluorescence staining of E17.5 embryos with anti- α SMA antibodies did reveal striking abnormalities in the structure of the ascending aorta, carotid and brachial arteries in *Itga5/av^{SM22-Cre}* mice. In control embryos, vSMCs appeared long, compact and were organised into 3-4 concentric lamellar units within the vessel wall (Fig. 3A,B). By contrast, vSMCs in the ascending aorta (data not shown) and right carotid/brachiocephalic artery of mutant embryos appeared round, disorganised and formed up to 18 layers of cells (Fig. 3C,D). Furthermore, in the most severely affected mutants, *Pecam1*-positive endothelial cells were undetectable within the aneurysm (Fig. 3C). Large regions of the great vessels appeared unaffected by the loss of both $\alpha 5$ and αv integrins however. vSMCs around the left carotid artery of *Itga5/av^{SM22-Cre}* embryos, for example, appeared well organised despite often displaying an increased number of lamellar units (supplementary material Fig. S6B). In addition, no

obvious defects in vSMC proliferation could be detected around the brachiocephalic or carotid arteries (supplementary material Fig. S7).

ECM deposition within the right brachiocephalic/carotid artery is disrupted in *Itga5/av^{SM22-Cre}* mutants

Previous studies have shown that the assembly of ECM proteins within the vessel wall is essential for maintaining the structural integrity of the great vessels. We therefore examined whether the dilated brachiocephalic/carotid artery in *Itga5/av^{SM22-Cre}* embryos was due to abnormal ECM deposition.

Surprisingly, despite the requirement for both $\alpha 5$ and αv integrins for fibronectin fibrillogenesis *in vitro*, fibronectin fibrils were clearly visible in the vessel walls of both early (supplementary material Fig. S8) and late (Fig. 4A) gestation *Itga5/av^{SM22-Cre}* embryos. In contrast to control mice, these fibrils displayed a disorganised lamellar organisation at E17.5 (Fig. 4A). The assembly of microfibril ECM proteins was also disrupted in *Itga5/av^{SM22-Cre}* embryos. In the dilated carotid arteries of mutant mice, fibrillin 1-containing microfibrils were almost undetectable in the tunica media, and organisation of fibulin 5 into lamellar structures appeared impaired (Fig. 4B,C). As observed in most human aneurysms, *Itga5/av^{SM22-Cre}* embryos also displayed elastin

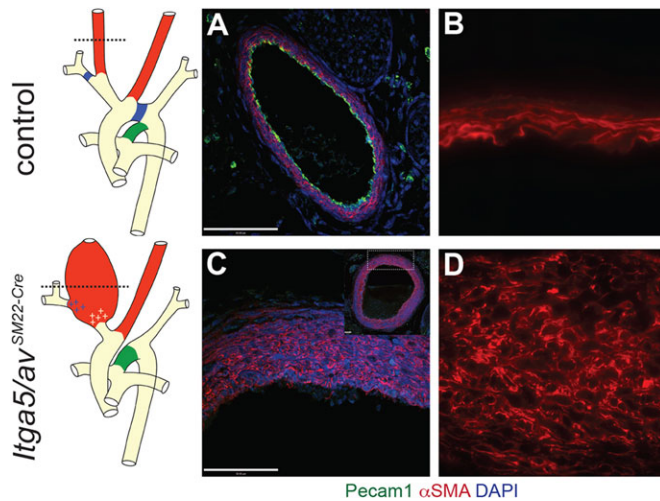


Fig. 3. Abnormal vSMC organisation in the brachiocephalic/carotid artery region of *Itga5/av*^{SM22-cre} embryos. (A–D) Transverse sections showing the structure of the right carotid artery in control (A,B) and *Itga5/av*^{SM22-cre} embryos (C,D) at E17.5. Inset in C shows the entire right carotid artery in section at lower magnification. (B,D) Higher magnification views of A,C. Note the abnormal thickening of arterial wall, and disorganised and round morphology of vSMCs in the *Itga5/av*^{SM22-cre} mutant. Scale bars: 50 μm in A,C.

fragmentation within their aneurysm (Fig. 4D). Furthermore, collagen IV fibrils, which are also found in the medial layers, were largely absent from the aneurysmal region of mutant mice (Fig. 4E). Thus, the disorganised pattern of vSMCs is accompanied by defects in organisation of several ECM proteins.

Loss of integrin α5 and αv disrupts focal adhesion formation and signalling via paxillin and FAK

To gain further insight into the molecular mechanisms underlying the *Itga5/av*^{SM22-cre} phenotype, vSMCs from the aortae of adult *Itga5/av*^{flox/flox} mice were isolated and immortalised with the SV40 large T antigen. vSMC identity was confirmed by immunofluorescence staining for αSMA and smoothelin (Fig. 5A). Integrin α5/αv-floxed cells were then infected with either an empty vector or

Cre-expressing adenovirus to generate control and integrin α5/αv-deficient vSMCs (*ΔItga5/av*), respectively. Efficient excision of the floxed alleles was confirmed by PCR (data not shown) and loss of both α5 and αv proteins verified by immunoblotting (Fig. 5B). Consistent with the binding affinities of α5 and αv, *ΔItga5/av* cells failed to attach to either fibronectin or vitronectin (Fig. 5C) and showed reduced adhesion to both laminin and collagen I substrates (supplementary material Fig. S9A), despite expressing similar levels of their cognate integrin receptors (supplementary material Fig. S9B). *ΔItga5/av* cells, however, adhered efficiently to Matrigel (Fig. 5C), but appeared smaller, more rounded and had fewer protrusions than control cells 24 h after plating (Fig. 6A–C).

Visualisation of the contacts between the cells and the ECM revealed that loss of both α5 and αv had dramatic effects on the formation of mature adhesions. In control vSMCs, focal adhesions are visible in cell protrusions and are present as fibrillar adhesions in the cell body (Fig. 6A,D). By contrast, *ΔItga5/av* cells contained only nascent adhesions and focal complexes throughout the cell (Fig. 6B,E). As a result, *ΔItga5/av* cells show reduced activation of the focal adhesion kinase (FAK/PTK2), markedly reduced levels of paxillin phosphorylation and reduced phosphorylation of the Crk-associated substrate p130 (CAS) (Fig. 6F; quantifications in supplementary material Fig. S9C). These deficits were rescued by re-expression of either *ITGA5* or *ITGAV* within *ΔItga5/av* cells (Fig. 6F), suggesting that either integrin can compensate for loss of the other.

Loss of α5 and αv integrins leads to abnormal TGF-β signalling

Given the similarity of the cardiovascular defects observed in *Itga5/av*^{SM22-cre} mutants and knockouts of *Ltbpl1* (Todorovic et al., 2007) or *TGFβ2* (Molin et al., 2004), and in mice in which the *Tgfr2* gene was conditionally ablated in vSMC precursors (Choudhary et al., 2009), we examined whether TGF-β signalling was disrupted in our *ΔItga5/av* cells. Immunoblotting for downstream mediators of the canonical TGF-β signalling pathway revealed that phosphorylation of SMAD2, but not of SMADs 1, 5 and 8 (Fig. 7A), was reduced in *ΔItga5/av* cells, despite a moderate increase in *Tgfb1* expression

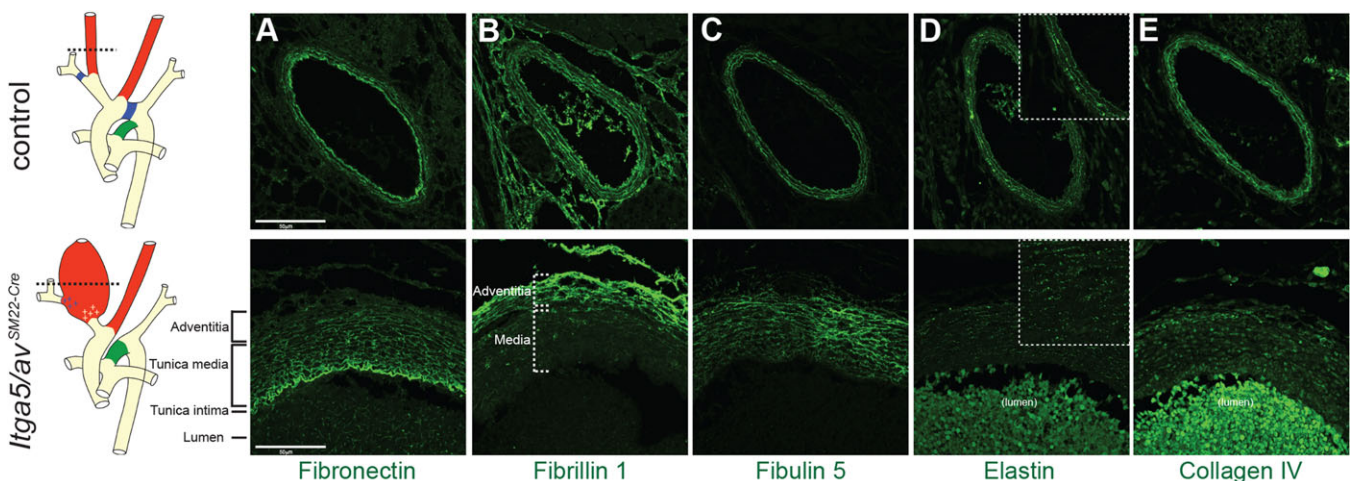


Fig. 4. Deposition of ECM proteins within the vessel wall of *Itga5/av*^{SM22-cre} embryos. (A–E) Immunofluorescence staining of transverse sections through the brachiocephalic/carotid artery of control and the corresponding dilated vessel of *Itga5/av*^{SM22-cre} embryos at E17.5, showing the deposition of (A) fibronectin, (B) fibrillin 1, (C) fibulin 5, (D) elastin (higher magnification views in insets) and (E) collagen IV; within the vessel wall. Note the concentric lamellar layers of ECM around the carotid artery in the control mouse (top), and the disorganised ECM within the tunica media in the mutant (bottom). The strong signals in the lumens in some panels arise from non-specific staining of blood cells. Scale bars: 50 μm in A for A–E.

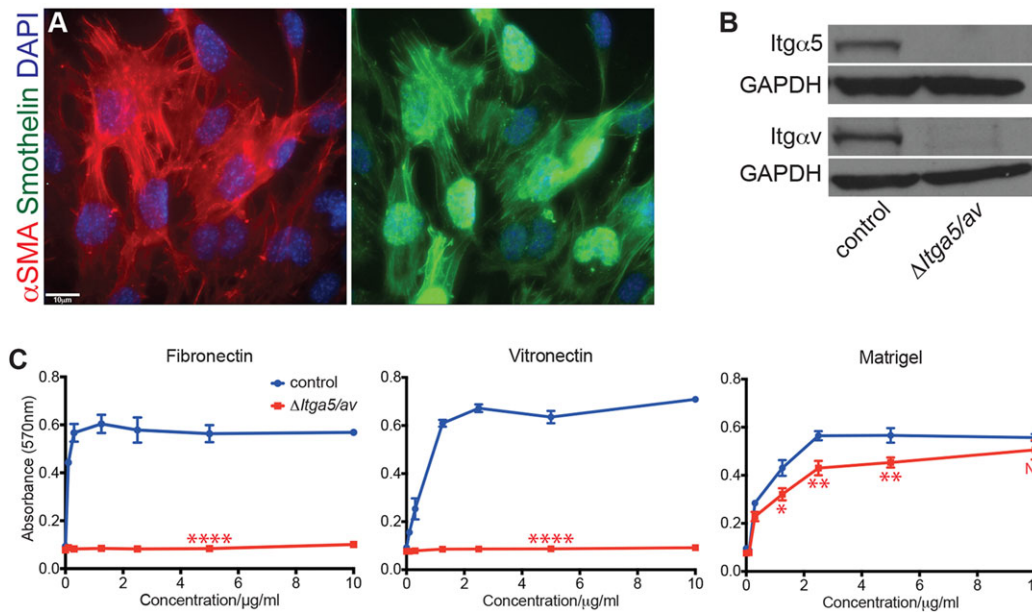


Fig. 5. Generation and characterisation of integrin $\alpha 5/\alpha v$ -deficient vSMCs. (A) Identity of vSMCs was confirmed by staining for α SMA (red) and smoothelin (green). (B) Western blots confirming efficient deletion of $\alpha 5$ and αv integrin subunits following Cre excision in $\Delta Itga5/av$ vSMCs. (C) Cell adhesion assay demonstrating the ability of $\Delta Itga5/av$ vSMCs to adhere to Matrigel, but not to fibronectin or vitronectin substrates. Results were analysed using Student's *t*-test and considered significant when * $P < 0.05$, ** $P < 0.01$ or **** $P < 0.0001$. Scale bar: 10 μ m in A.

(supplementary material Fig. S9D). The extent of this reduction in SMAD signalling appeared dependent on the Matrigel batch used, with some experiments producing only small changes in the level of pSMAD2 on specific Matrigel preparations (data not shown). To our surprise, immunofluorescence staining revealed that pSMAD2 levels were increased in the aneurysmal region of $Itga5/av^{SM22-Cre}$ embryos, when compared with the right carotid artery of control E17.5 mice (Fig. 7B). Interestingly, this increase was also apparent, just before the onset of the large dramatic aneurysm, in the brachiocephalic/carotid region in E12.5 embryos (supplementary material Fig. S10). However, no obvious differences in pSMAD2 signalling were observed in any of the other regions of $Itga5/av^{SM22-Cre}$ embryos examined (Fig. 7B).

$\alpha 5\beta 1$ and αv integrins bind to the latency-associated protein (LAP)

TGF- β is secreted as an inactive form and requires release from LAP to exert its biological functions. Previous studies have shown that integrins regulate TGF- β signalling by interacting with the RGD motif contained in the LAPs of TGF- $\beta 1$ and TGF- $\beta 3$, thus releasing TGF- β from its latent complex (Munger et al., 1999; Annes et al., 2002; Yang et al., 2007). To determine whether loss of both $\alpha 5$ and αv prevented binding to LAP, we assessed the ability of control, $\Delta Itgav$, $\Delta Itga5$ and $\Delta Itga5/av$ vSMCs to adhere to recombinant human TGF- $\beta 1$ LAP-coated plates. Consistent with previous data (Munger et al., 1998, 1999; Ludbrook et al., 2003), loss of integrin αv significantly reduced binding to LAP (Fig. 7C). Adhesion to LAP was also reduced in $\Delta Itga5$ vSMCs, albeit to a lesser extent than in $\Delta Itgav$ cells, whereas binding to LAP was almost completely blocked in cells lacking both $\alpha 5$ and αv integrins (Fig. 7C).

Integrin $\alpha 5$ and αv are required for incorporation of Ltpb1 but not Ltpb3 into the ECM

Integrin binding to LAP alone is insufficient for TGF- β activation. The complex of TGF- β and LAP (small latent complex) also requires

anchoring to the ECM through its association with Ltpb1 and Ltpb3 (Horiguchi et al., 2012). For Ltpb1, this incorporation is dependent on the assembly of fibronectin, and is independent of fibrillin expression, whereas incorporation of Ltpb3 is dependent on assembly of fibrillin 1 microfibrils (Zilberberg et al., 2012). To examine whether $\Delta Itga5/av$ vSMCs could incorporate Ltpb1 into the matrix, we first analysed the ability of $\Delta Itga5/av$ vSMCs to assemble endogenous fibronectin into fibrils. Immunofluorescence staining revealed that control vSMCs form extensive fibronectin fibrils 24 h after plating (Fig. 7D). By contrast, $\Delta Itga5/av$ vSMCs plated at confluency formed smaller aggregates of fibronectin (Fig. 7D). As fibronectin mRNA expression levels were reduced (30–40%) in cells lacking both $\alpha 5$ and αv (supplementary material Fig. S11A), we analysed the ability of $\Delta Itga5/av$ vSMCs to incorporate exogenous biotin-labelled fibronectin into the DOC-insoluble matrix (supplementary material Fig. S11B). This revealed that, even after 5 days in culture, $\Delta Itga5/av$ vSMCs are unable to assemble exogenous fibronectin into fibrils (supplementary material Fig. S11B). Re-expression of either $\alpha 5$ or αv integrin, however, rescued the ability of $\Delta Itga5/av$ vSMCs to assemble and incorporate fibronectin into the DOC-insoluble matrix (Fig. 7E). Similarly, $\Delta Itga5/av$ vSMCs also had defects in their ability to assemble the RGD-containing microfibrillar proteins fibrillin 1 and fibulin 5 *in vitro* (Fig. 7E). Surprisingly, in contrast to our *in vivo* results, lack of fibrillin 1 and fibulin 5 did not affect the deposition of elastin (Fig. 7E). Loss of $\alpha 5$ and αv integrins did affect incorporation of the RGD-containing Ltpb1 into the DOC-insoluble matrix however (Fig. 7F). After 3 days in culture, Ltpb1 was incorporated into the ECM by control, and to a lesser extent $\Delta Itga5$ and $\Delta Itgav$ vSMCs, but was completely absent from the ECM assembled by $\Delta Itga5/av$ cells (Fig. 7F). Interestingly, incorporation of Ltpb3, which does not contain an RGD motif, appeared unaffected by loss of $\alpha 5$ and αv and the lack of fibronectin and fibrillin 1 fibrils (Fig. 7F). Thus, absence of these two integrin subunits on vSMCs compromises assembly of ECM proteins and components of TGF- β signalling complexes.

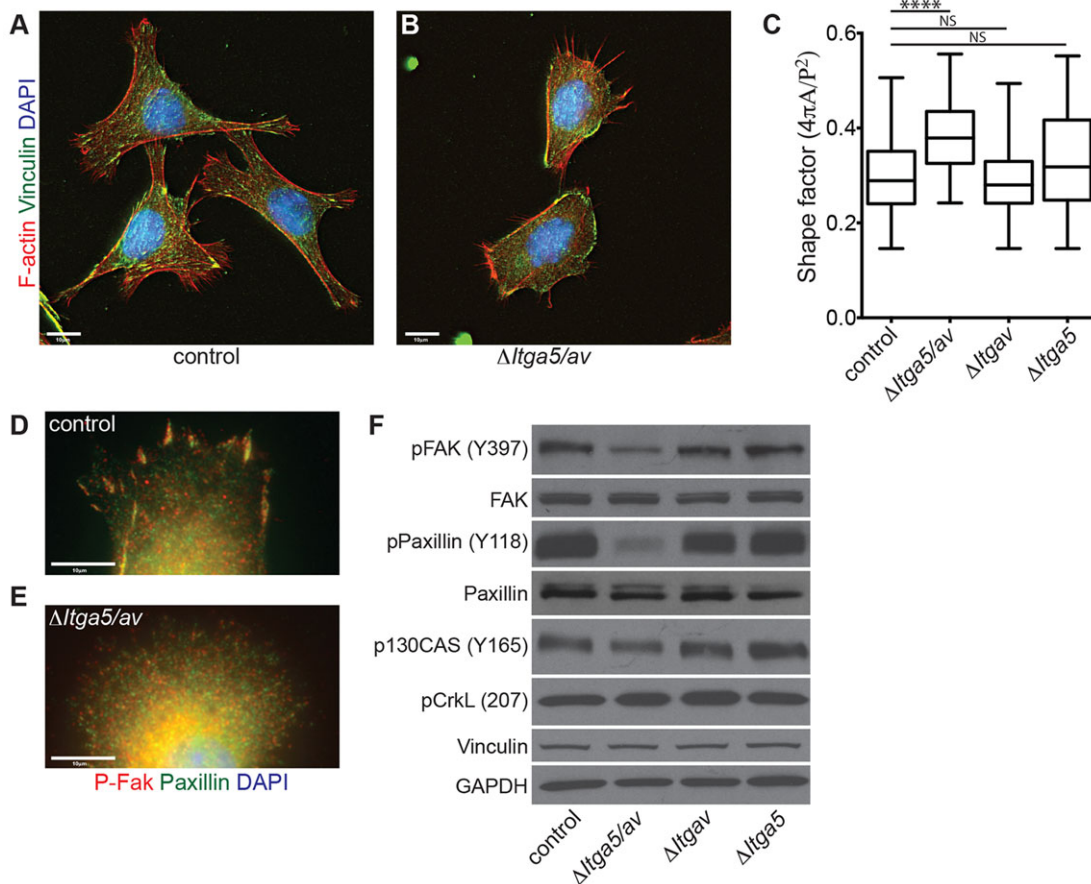


Fig. 6. Abnormal focal adhesion formation in $\Delta Itga5/av$ vSMCs. (A,B) Double-immunofluorescence staining showing the actin cytoskeleton (red) and distribution of focal adhesions (vinculin, green) in control (A) and $\Delta Itga5/av$ vSMCs (B) plated on Matrigel for 24 h. Note the more rounded morphology and lack of cellular protrusions in $\alpha 5/\alpha v$ -deficient vSMCs. (C) Cell-shape analysis of control, $\Delta Itgav$, $\Delta Itga5$ and $\Delta Itga5/av$ vSMCs. An increased shape factor for $\Delta Itga5/av$ vSMCs indicates a less complex, more rounded cell shape. **** $P < 0.0001$; Student's *t*-test. (D,E) Focal adhesion organisation in the lamellipodia of control (D) and $\Delta Itga5/av$ vSMCs (E) as seen by immunofluorescence for phospho-FAK (red) and paxillin (green). $\Delta Itga5/av$ vSMCs form only nascent adhesions and focal contacts, whereas control cells form large focal adhesions. (F) Western blots showing that $\Delta Itga5/av$ vSMCs have reduced levels of phosphorylation of FAK, paxillin and p130Cas. These reduced levels are rescued by re-expression of either $\alpha 5$ ($\Delta Itgav$) or αv integrin ($\Delta Itga5$). Scale bars: 10 μ m in A,B,D,E.

DISCUSSION

In this study, we have shown that $\alpha 5$ and αv integrins on neural crest-derived vSMCs cooperate to control remodelling of the PAAs, and are essential for the septation of the heart and outflow tract. We have also shown that vSMC expression of both $\alpha 5$ and αv subunits are essential for assembly of ECM within the vessel wall, and that loss of both integrins leads to the formation of large aneurysms within the brachiocephalic/carotid arteries. Expression of $\alpha 5$ and αv integrins, however, appears to be dispensable for the initial assembly of an extensive vascular network and the function of vSMCs surrounding vessels in the skin.

Cardiovascular development is regulated by $\alpha 5$ and αv integrins

Consistent with our previous study (Turner et al., 2014), genetic ablation of $\alpha 5\beta 1$ from vSMCs failed to replicate any of the vascular defects observed in the global *Itga5* KO mice (Yang et al., 1993; Francis et al., 2002). *Itga5^{SM22-Cre}* mice survived to birth with no obvious vSMC or cardiovascular defects. Similarly, despite numerous studies suggesting that αv integrins play a key role in controlling vSMC function *in vitro* (Liaw et al., 1995; D'Angelo et al., 1997; Panda et al., 1997; Dahm and Bowers, 1998), *Itgav^{SM22-Cre}* mutants developed normally and contained blood vessels

indistinguishable from those in control mice. However, both *Itga5^{SM22-Cre}* and *Itgav^{SM22-Cre}* mice displayed postnatal lethality, suggesting that loss of either integrin increases susceptibility to cardiovascular defects after birth. Although contradictory to numerous blocking studies *in vitro*, the lack of major vascular defects in *Itga5^{SM22-Cre}* and *Itgav^{SM22-Cre}* embryos fits with a growing body of data showing that $\alpha 5$ and αv integrins have overlapping functions and that either integrin can compensate for loss of the other (Yang and Hynes, 1996; Takahashi et al., 2007; van der Flier et al., 2010). Indeed, ablation of *Itga5* or *Itgav* alone caused only a minor reduction in focal adhesion signalling and matrix assembly in our cultured vSMCs. It is also possible that some integrin functions, such as assembly of ECM matrix or activation of TGF- β , are compensated for by integrins expressed on adjacent cells within the vasculature. This might help explain why tissue-specific integrin mutants often display phenotypes less severe than those predicted from *in vitro* studies.

In contrast to the results for single *Itga5^{SM22-Cre}* and *Itgav^{SM22-Cre}* mutants, deletion of both $\alpha 5$ and αv integrins by *SM22 α -Cre* caused significant cardiovascular defects. *Itga5/av^{SM22-Cre}* embryos developed interrupted aortic arch type-B and a large aneurysm that encompassed the brachiocephalic artery and the proximal region of the right carotid artery. The same phenotype has been

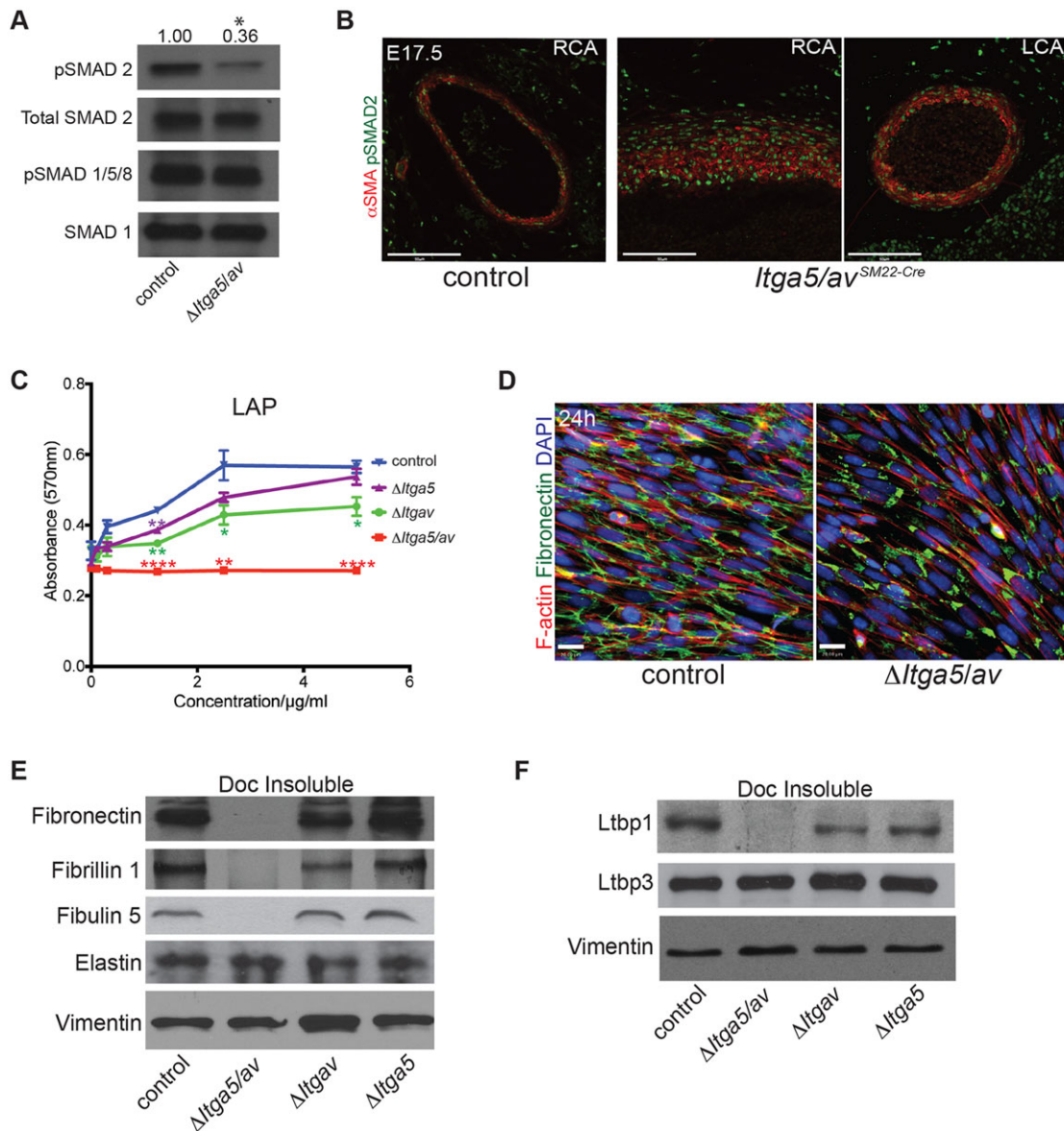


Fig. 7. TGF- β activation is mediated via $\alpha 5$ and αv integrins. (A) Western blot showing that phosphorylation of SMAD2, but not of SMAD1/5/8, is reduced in $\Delta Itga5/av$ vSMCs plated on Matrigel. (B) Immunofluorescence staining showing the level of pSMAD2 expression in the carotid arteries of control and $Itga5/av^{SM22-Cre}$ embryos at E17.5. Note that pSMAD2 levels are increased within the dilated right carotid artery (RCA) compared with the left carotid artery (LCA) of the mutant embryos. (C) Cell adhesion to the LAP of TGF- β 1 is inhibited in $\Delta Itga5/av$ cells. * $P < 0.05$, ** $P < 0.01$ or **** $P < 0.001$; Student's t -test. (D) $\Delta Itga5/av$ cells are less able to assemble fibronectin (green) into fibrils or incorporate fibronectin, fibrillin 1 or fibulin 5 into the DOC-insoluble matrix (E). Note that despite the loss of fibrillin 1 and fibulin 5 assembly, elastin is still incorporated into the matrix by $\Delta Itga5/av$ cells (E). (F) Incorporation of Ltpb1, but not of Ltpb3, into the DOC-insoluble matrix is inhibited by the loss of $\alpha 5$ and αv integrins. Scale bars: 50 μm in B; 20 μm in D.

observed in mice that lack vSMC expression of all the $\beta 1$ integrins (Turlo et al., 2012). This suggests that the phenotype of $Itga5/av^{SM22-Cre}$ mice, and therefore the vSMC-specific $Itgb1$ mutant, is caused by the loss of $\alpha 5\beta 1$ and specifically $\alpha v\beta 1$, rather than any of the other αv ($\alpha v\beta 3$, $\alpha v\beta 5$, $\alpha v\beta 6$ and $\alpha v\beta 8$) or $\beta 1$ ($\alpha 1\beta 1$, $\alpha 2\beta 1$, $\alpha 3\beta 1$, $\alpha 4\beta 1$, $\alpha 6\beta 1$, $\alpha 7\beta 1$, $\alpha 9\beta 1$, $\alpha 10\beta 1$, $\alpha 11\beta 1$) integrin heterodimers. Like Turlo et al. (2012), we also found that migration and initiation of vSMC fate were unaffected by loss of $\alpha 5$ and αv integrins. vSMCs in $Itga5/av$ mutants expressed high levels of the vSMC markers αSMA , SM22 α and Myh11, and migrated efficiently to the PAAs and blood vessels within the skin. Deletion of both $\alpha 5$ and αv integrins also appeared to have no obvious effect on the functions of mesodermally derived vSMCs during embryonic development. In contrast to mural cell-specific $Itgb1$ mutant mice (Abraham et al.,

2008), in which vSMCs appeared round, poorly spread and only loosely attached to the subendothelial basement membrane, vSMCs in the cutaneous vasculature of $Itga5/av^{SM22-Cre}$ embryos appeared indistinguishable from those in control mice. One possible explanation for these conflicting results is that vascular defects in mural cell-specific $\beta 1$ mutants are due to loss of $Itgb1$ on pericytes, rather than vSMCs. Alternatively, $\beta 1$ heterodimers, other than $\alpha 5\beta 1$ and $\alpha v\beta 1$, might play important roles in mesodermally derived vSMCs; defects in pericyte and vSMC distribution have been reported in $\alpha 4$ and $\alpha 7$ -KO mice (Flintoff-Dye et al., 2005; Garmy-Susini et al., 2005; Grazioli et al., 2006). Arguing against this latter hypothesis, however, is the fact that vascular defects also appear to be restricted to areas populated by neural-crest-derived vSMCs in mice in which $Itgb1$ has been deleted in all vSMCs, using the same

SM22 α -Cre line as in this study (Turlo et al., 2012). Nevertheless, large aneurysms are found both in $\beta 1$ mutants (Abraham et al., 2008; Turlo et al., 2012) and in our *Itga5/av^{SM22-Cre}* embryos. As in the vSMC-specific $\beta 1$ mutants (Turlo et al., 2012), aneurysms were present only in the brachiocephalic and carotid arteries. This could be due to these regions exhibiting the greatest shear stress (Meng et al., 2007; Huo et al., 2008; Wang et al., 2009), especially when flow is redirected to the brachiocephalic and right carotid artery when the aortic arch is interrupted. These regions of the vasculature also correlate with areas of maximum integrin $\beta 1$ expression (Turlo et al., 2012). It is therefore possible that the aorta, brachiocephalic and carotid artery are more sensitive to the loss of *Itga5* and *Itgav*, and might suggest that both $\alpha 5\beta 1$ and $\alpha v\beta 1$ integrins play an important role in providing structural strength to the blood vessels and in resisting the high pulsatile flow from the heart. Alternatively, these regions might be more susceptible, due to being populated by different subsets of CNCCs, compared with other parts of the great vessels, and heightened expression of $\beta 1$ integrins might simply correlate with a specific population of vSMCs. Interestingly, decreased expression of *ITGA5* has previously been linked to formation of human aortic aneurysms (Cheuk and Cheng, 2004), and, similar to some human aneurysms (Pera et al., 2010) and experimentally induced aneurysms in mice (Murphy and Hynes, 2014), *Pecam1*-positive endothelial cells were reduced in the dilated brachiocephalic artery of *Itga5/av^{SM22-Cre}* mice at late stages. It is unclear, however, whether this loss is specifically linked to deletion of both $\alpha 5$ and αv within vSMCs, or merely part of the general pathology occurring within a large aneurysm. It is conceivable that defects in vSMC function (assembly of the basement membrane ECM, signalling, contraction) are directly, or indeed indirectly, causing this dedifferentiation. After all, mechanosensing by *Pecam1* is directly linked to integrin engagement to the ECM (Collins et al., 2012), *Pecam1* is a ligand for $\alpha v\beta 3$ (Piali et al., 1995) and is regulated by TGF- β (Neubauer et al., 2008).

As *SM22 α -Cre* is also expressed in the heart (Turlo et al., 2012), we cannot definitively rule out the possibility that the *Itga5/av^{SM22-Cre}* phenotype is secondary to heart defects. Development of the aortic arch has been shown to be linked to the haemodynamics of blood flowing from the heart (Yashiro et al., 2007). However, as septation and PTA defects were also found in *Itga5/av^{Wnt1-Cre}* embryos, which lacked aneurysms and aortic arch defects, and because *Itga5/av^{SM22-Cre}* mice developed dilated brachiocephalic/carotid arteries before cardiac septation at E12.5, we think that this is unlikely. We believe instead, as both neural crest and mesenchyme-derived cells contribute to the aorta and PAAs (Bergwerff et al., 1998), that the vascular defects are less severe in *Itga5/av^{Wnt1-Cre}* embryos, as $\alpha 5/\alpha v$ -containing mesenchyme-derived cells can compensate, at least in part, for the loss of both integrins in the neural-crest-derived vSMCs.

$\alpha 5$ and αv integrins are essential for neural crest functions *in vivo*

In our attempts to further understand the cardiovascular defects in our mutants, we have also investigated the ways in which $\alpha 5$ and αv integrins cooperate to regulate neural crest function. Almost all *Itga5^{Wnt1-Cre}* embryos died shortly after birth, whereas *Itgav^{Wnt1-Cre}* and, to a greater extent, *Itga5/av^{Wnt1-Cre}* mutants, displayed perinatal lethality. The loss of *Itga5/av^{Wnt1-Cre}* mice is considerably later than the lethality seen in neural crest-specific *Itgb1* mutants (Turlo et al., 2012), confirming the importance of other $\beta 1$ -containing receptors in neural crest cells. Both cardiac and cranial neural crest defects were observed in *Itga5/av^{Wnt1-Cre}* mutants. In addition to developing

a PTA and ventricular septation defects (VSDs), *Itga5/av^{Wnt1-Cre}* mice also displayed mislocated thymi and cleft palates. Previous studies have shown that migration of neural crest cells is dependent on $\alpha 5$ and αv expression, and defects in neural crest migration can lead to heart, thymus and craniofacial defects (Delannet et al., 1994; Alfandari et al., 2003; Keyte and Hutson, 2012). Migration defects do not appear to be the cause, at least of the cardiovascular defects, in *Itga5/Itgav^{Wnt1-Cre}* mutants. Although we cannot rule out relatively subtle defects in the migration of specific subsets of neural crest cells, *Wnt1*-positive CNCCs were clearly present in the PAA and outflow tracts in *Itga5/Itgav^{Wnt1-Cre}* embryos as early as E11.5. These results are consistent with a number of studies showing that septation and PAA defects can occur independently from neural crest migration and differentiation defects (Molin et al., 2004; Turlo et al., 2012).

Role of $\alpha 5$ and αv integrins in cardiovascular development

So how do $\alpha 5$ and αv integrins regulate cardiovascular development? Our analysis of Δ *Itga5/av* vSMCs *in vitro* suggests a number of possibilities. First, our data show that loss of the $\alpha 5$ and αv integrins prevents the formation of mature focal adhesions and, as a consequence, leads to reduced levels of FAK and paxillin phosphorylation. Focal adhesions are essential for maintaining structural integrity of vessels by inducing cytoskeletal rearrangements and alignment of vSMCs in response to mechanical strain. Previous studies have shown that genetic deletion of FAK (*Ptk2*) in vSMC precursors leads to defects in the patterning of the aortic arch arteries and septation of the heart and outflow tract (Hakim et al., 2007; Vallejo-Illarramendi et al., 2009; Cheng et al., 2011). These defects, however, are caused by abnormal recruitment (Hakim et al., 2007; Cheng et al., 2011) and/or impaired differentiation of vSMCs (Vallejo-Illarramendi et al., 2009), neither of which was seen in our mutants. Less information exists about the role of paxillin in vSMCs. *In vitro*, paxillin has been implicated in regulating adhesion, proliferation, apoptosis and activation of L-type calcium channels in vSMCs (Wu et al., 2001; Veith et al., 2012). To date, no one has investigated the role of paxillin specifically in vSMCs *in vivo*. Intriguingly, however, paxillin KO mice die at E9.5 with cardiac and somitic defects resembling those in fibronectin KO mice (Hagel et al., 2002).

The cardiovascular defects in *Itga5/av^{SM22-Cre}* mice might also be due to the inability of Δ *Itga5/av* vSMCs to interact correctly with the ECM. Δ *Itga5/av* vSMCs failed to attach to either fibronectin or vitronectin and displayed reduced adhesion to laminin and collagen I. As a result, Δ *Itga5/av* vSMCs often appeared poorly spread *in vitro* and mirrored the round, disorganised morphology of vSMCs within the ascending aorta, brachiocephalic and right carotid artery of *Itga5/av^{SM22-Cre}* embryos. Our data also indicate that $\alpha 5$ and αv integrins are required for the assembly and organisation of the ECM within the vessel wall. *In vitro*, consistent with $\alpha 5$ and αv being the predominant RGD-binding receptors expressed on vSMCs, Δ *Itga5/av* vSMCs were unable to incorporate fibronectin, fibrillin 1 or fibulin 5 into the DOC-insoluble ECM. Furthermore, organisation of the ECM into concentric lamellar layers around the ascending aorta, brachiocephalic and carotid artery appeared severely compromised in *Itga5/av^{SM22-Cre}* mice. Correct assembly of the ECM is essential for maintaining vascular integrity; vSMCs alone are insufficient to resist the mechanical strain generated by pulsatile blood flow (Wagenseil and Mecham, 2009). Defects in assembly of fibrillin, fibulin, collagen and elastin have all been implicated in the formation of aneurysms *in vivo* (El-Hamamsy and Yacoub, 2009). It is therefore probable that the

abnormal assembly of the ECM weakens the vessel wall and directly causes the aneurysms in *Itga5/av*^{SM22-Cre} embryos.

A final intriguing possibility is that the defects in *Itga5/av*^{SM22-Cre} mice are in fact related to abnormal TGF- β signalling. Previous studies have shown that TGF- β signalling is essential for the patterning of the aortic arch, septation of the heart and outflow tract, and for fusion of the palatal shelves and development of the thymus (Ito et al., 2003; Molin et al., 2004; Wang et al., 2006; Todorovic et al., 2007; Choudhary et al., 2009), defects all present in our *Itga5/Itgav* mutants. Furthermore, Δ *Itga5/av* vSMCs were unable to bind to LAP or to deposit *Ltbp1* into the ECM, and had decreased levels of pSMAD2. Paradoxically, *in vivo*, *Itga5/av*^{SM22-Cre} mice displayed increased levels of pSMAD2 within their aneurysms. This ‘TGF- β paradox’ has also been seen in aortic aneurysms present in patients with Loeys–Dietz and Marfan’s syndromes, which, in theory, should also exhibit reduced pSMAD2 levels within their vasculature (Lin and Yang, 2010). The exact mechanism for this paradox remains unclear. However, it might be due to excessive (compensatory) upregulation of TGF- β , increased metalloproteinase expression, dysregulation of TGF- β signalling-feedback loops, or even through non-TGF- β activators of SMADs (Lin and Yang, 2010). There is also the possibility that the defects in *Itga5/av*^{SM22-Cre} mice are actually due to reduced non-SMAD TGF- β signalling (Moustakas and Heldin, 2005). As there is extensive cross-talk between TGF- β signalling pathways, integrins, focal adhesions and the ECM, it is extremely difficult to unravel the exact chain of causality leading to the defects seen in *Itga5/av*^{SM22-Cre} mice or those in TGF- β signalling.

Role of $\alpha 5$ and αv integrins in initial development of blood vessels

Deletion of both $\alpha 5$ and αv integrins from either vSMCs or endothelial cells results in defects in the remodelling of the great vessels and the heart, but, in both cases, fails to disrupt initial blood vessel development (van der Flier et al., 2010; Turner et al., 2014), or replicate the phenotypes of the global KO mice. These observations suggest that integrins on both mural cells (pericytes, vSMCs) and endothelial cells cooperate to regulate the assembly of ECM proteins and signalling complexes such as those for TGF- β within the ECM. It is, of course, possible that some other cell types expressing these integrins play some essential role, although this seems to us less likely.

Conclusions

Congenital heart defects (CHD) are a leading cause of miscarriage and the most common type of birth defect (Bruneau, 2008). Furthermore, as surgical intervention has advanced, and more children with CHD survive into adulthood, there is an even greater need to understand the molecular pathways that regulate cardiovascular development. Our study has shown that $\alpha 5$ and αv integrins are essential for development of the heart and great vessels. However, many questions about their precise roles in vascular development and homeostasis remain unresolved. Future experiments will need to examine the role of $\alpha 5$ and αv integrins in the adult vasculature, and assess whether loss of either integrin subunit increases susceptibility to aortic aneurysms and other vascular diseases.

MATERIALS AND METHODS

Mouse lines

All mouse strains were on 129S4:C57BL/6 mixed background. *Itga5* floxed (van der Flier et al., 2010), *Itgav* floxed (Lacy-Hulbert et al., 2007), mTmG (Muzumdar et al., 2007), Rosa *lacZ* (Soriano, 1999), *SM22 α -Cre*

(Holtwick et al., 2002) and *Wnt1-Cre* (Danielian et al., 1998) mouse lines have all been described previously. Genotyping was performed on DNA isolated from tail snips in house or by Transnetyx. All mice were housed and handled in accordance with approved Massachusetts Institute of Technology Division of Comparative Medicine protocols (IACUC approval 0412-033-15).

Micro-CT scans

4% PFA-fixed embryos were sent to Numira Biosciences for micro-CT imaging. Specimens were stained with a proprietary contrast agent. A high-resolution volumetric micro-CT scanner (μ CT40; Scanco Medical) was used to scan the tissue (6 μ m isometric voxel resolution, 200 ms exposure, 2000 views and 5 frames per view). The micro-CT generated DICOM files, which were analysed using OsiriX and Volocity software.

vSMC isolation and culture

vSMCs were isolated from the aortic arch and carotid arteries of *Itga5*^{fllox/fllox}; *Itgav*^{fllox/fllox} mice as per Ray et al. (2001) (see supplementary materials and methods). Upon confirmation of vSMC identity by α SMA- and smoothelin-positive immunofluorescence staining, cells were immortalised using SV40 large T antigen (Zhao et al., 2003) and infected with either empty vector or Cre-expressing adenovirus to generate control or $\alpha 5/\alpha v$ -deficient vSMCs (Δ *Itga5/av*), respectively. Following excision, both control and Δ *Itga5/av* cells were grown on plates coated with 20 μ g/ml Matrigel (BD Bioscience). To generate vSMCs lacking either $\alpha 5$ or αv integrins, Δ *Itga5/av* cells were infected with retroviral constructs containing *ITGAV* or *ITGA5* (van der Flier et al., 2010) to generate Δ *Itga5* or Δ *Itgav* cells, respectively.

Cell adhesion assays

96-well plates were coated overnight at 4°C with serial dilutions of fibronectin, collagen I, laminin, vitronectin, Matrigel or recombinant human LAP (TGF- $\beta 1$) (R&D Systems). After blocking with 5% BSA, 20,000 cells/well were plated and allowed to adhere for 24 h. Unattached cells were removed by aspiration, and adherent cells were fixed with 4% PFA and stained with 0.1% Crystal Violet. To quantify adhesion, cells were permeabilised in 50 μ l of PBS/0.2% Triton X-100, and OD₅₉₀ was measured in a plate reader.

Cell shape analysis

Cells were seeded at low density and allowed to adhere to Matrigel-coated glass coverslips for 24 h. The cells were then fixed and stained with phalloidin and DAPI. Following imaging of six fields from each coverslip, images were automatically analysed using Volocity software to detect the outline of the cells. Cells touching other cells or the border of the image were rejected from the analysis, and the shape factor was calculated using the formula ($4 \times \pi \times \text{area} / \text{perimeter}^2$). A circular cell shape will give a factor of 1, whereas a complex cell shape will give values closer to 0.

DOC insolubility assays

vSMCs were seeded at confluence (200,000 cells/ml) on Matrigel-coated plates in fibronectin-depleted medium in the presence or absence of exogenous biotinylated human fibronectin (10 μ g/ml). At 1, 3 and 5 days post plating, medium was collected, and cells were lysed in 0.5 ml DOC buffer [2 mM EDTA, 1% sodium deoxycholate, 20 mM Tris pH 8.5, complete mini-protease inhibitors (Roche)] for fibronectin experiments or in 0.25% DOC for investigation of *Ltbp1* incorporation into the insoluble matrix fraction. After passing eight times through a 22 G needle, DOC-insoluble material was spun down for 20 min at 20,000 *g* at 4°C and solubilized in 120 μ l 2 \times reducing SDS-PAGE loading buffer. Reduced (100 mM DTT) samples were loaded onto 4–12% gels.

See supplementary materials and methods for details of histology, immunofluorescence staining, immunoblotting and RT-qPCR.

Acknowledgements

We thank members of the Hynes laboratory, especially Patrick Murphy, for discussions and advice.

Competing interests

The authors declare no competing or financial interests.

Author contributions

Experiments were conceived, designed and interpreted by C.J.T., K.B.-N., A.v.d.F. and R.O.H. Experiments were performed by C.J.T., K.B.-N. and A.v.d.F.; D.C. provided sections. The manuscript was written by C.J.T. and R.O.H.

Funding

This work was supported by grants from the National Institutes of Health [PO1-HL66105 to Monty Krieger, PI], the National Institute of General Medical Sciences (NIGMS) Cell Migration Consortium [GC11451.126452, to A. F. Horwitz, PI] and by the Koch Institute Support (core) [Grant P30-CA14051] from the National Cancer Institute and the Howard Hughes Medical Institute (HHMI). C.J.T. was a postdoctoral associate and R.O.H. is an Investigator of the HHMI. Deposited in PMC for release after 6 months.

Supplementary material

Supplementary material available online at

<http://dev.biologists.org/lookup/suppl/doi:10.1242/dev.117572/-/DC1>

References

- Abraham, S., Kogata, N., Fassler, R. and Adams, R. H. (2008). Integrin beta1 subunit controls mural cell adhesion, spreading, and blood vessel wall stability. *Circ. Res.* **102**, 562-570.
- Alfandari, D., Cousin, H., Gaultier, A., Hoffstrom, B. G. and DeSimone, D. W. (2003). Integrin alpha5beta1 supports the migration of *Xenopus* cranial neural crest on fibronectin. *Dev. Biol.* **260**, 449-464.
- Annes, J. P., Rifkin, D. B. and Munger, J. S. (2002). The integrin alphaVbeta6 binds and activates latent TGFbeta3. *FEBS Lett.* **511**, 65-68.
- Astrof, S. and Hynes, R. O. (2009). Fibronectins in vascular morphogenesis. *Angiogenesis* **12**, 165-175.
- Bader, B. L., Rayburn, H., Crowley, D. and Hynes, R. O. (1998). Extensive vasculogenesis, angiogenesis, and organogenesis precede lethality in mice lacking all alphaV integrins. *Cell* **95**, 507-519.
- Barillari, G., Albonici, L., Incerpi, S., Bogetto, L., Pistrutto, G., Volpi, A., Ensolì, B. and Manzari, V. (2001). Inflammatory cytokines stimulate vascular smooth muscle cells locomotion and growth by enhancing alpha5beta1 integrin expression and function. *Atherosclerosis* **154**, 377-385.
- Bergwerff, M., Verberne, M. E., DeRuiter, M. C., Poelmann, R. E. and Gittenberger-de Groot, A. C. (1998). Neural crest cell contribution to the developing circulatory system: implications for vascular morphology? *Circ. Res.* **82**, 221-231.
- Bruneau, B. G. (2008). The developmental genetics of congenital heart disease. *Nature* **451**, 943-948.
- Cheng, Z., Sundberg-Smith, L. J., Mangiante, L. E., Sayers, R. L., Hakim, Z. S., Musunuri, S., Maguire, C. T., Majesky, M. W., Zhou, Z., Mack, C. P. et al. (2011). Focal adhesion kinase regulates smooth muscle cell recruitment to the developing vasculature. *Arterioscler. Thromb. Vasc. Biol.* **31**, 2193-2202.
- Cheuk, B. L. Y. and Cheng, S. W. K. (2004). Differential expression of integrin alpha5beta1 in human abdominal aortic aneurysm and healthy aortic tissues and its significance in pathogenesis. *J. Surg. Res.* **118**, 176-182.
- Choudhary, B., Zhou, J., Li, P., Thomas, S., Kaartinen, V. and Sucov, H. M. (2009). Absence of TGFbeta signaling in embryonic vascular smooth muscle leads to reduced lysyl oxidase expression, impaired elastogenesis, and aneurysm. *Genesis* **47**, 115-121.
- Collins, C., Guilluy, C., Welch, C., O'Brien, E. T., Hahn, K., Superfine, R., Burrige, K. and Tzima, E. (2012). Localized tensional forces on PECAM-1 elicit a global mechanotransduction response via the integrin-RhoA pathway. *Curr. Biol.* **22**, 2087-2094.
- Dahm, L. M. and Bowers, C. W. (1998). Vitronectin regulates smooth muscle contractility via alphaV and beta1 integrin. *J. Cell Sci.* **111**, 1175-1183.
- Danielian, P. S., Muccino, D., Rowitch, D. H., Michael, S. K. and McMahon, A. P. (1998). Modification of gene activity in mouse embryos in utero by a tamoxifen-inducible form of Cre recombinase. *Curr. Biol.* **8**, 1323-1326.
- Davenpeck, K. L., Marcinkiewicz, C., Wang, D., Niculescu, R., Shi, Y., Martin, J. L. and Zaleski, A. (2001). Regional differences in integrin expression: role of alpha(5)beta(1) in regulating smooth muscle cell functions. *Circ. Res.* **88**, 352-358.
- Delannet, M., Martin, F., Bossy, B., Cheresch, D. A., Reichardt, L. F. and Duband, J. L. (1994). Specific roles of the alpha V beta 1, alpha V beta 3 and alpha V beta 5 integrins in avian neural crest cell adhesion and migration on vitronectin. *Development* **120**, 2687-2702.
- D'Angelo, G., Mogford, J. E., Davis, G. E., Davis, M. J. and Meininger, G. A. (1997). Integrin-mediated reduction in vascular smooth muscle [Ca²⁺]_i induced by RGD-containing peptide. *Am. J. Physiol.* **272**, H2065-H2070.
- El-Hamamsy, I. and Yacoub, M. H. (2009). Cellular and molecular mechanisms of thoracic aortic aneurysms. *Nat. Rev. Cardiol.* **6**, 771-786.
- Flintoff-Dye, N. L., Welsler, J., Rooney, J., Scowen, P., Tamowski, S., Hatton, W. and Burkin, D. J. (2005). Role for the alpha7beta1 integrin in vascular development and integrity. *Dev. Dyn.* **234**, 11-21.
- Foo, S. S., Turner, C. J., Adams, S., Compagni, A., Aubyn, D., Kogata, N., Lindblom, P., Shani, M., Zicha, D. and Adams, R. H. (2006). Ephrin-B2 controls cell motility and adhesion during blood-vessel-wall assembly. *Cell* **124**, 161-173.
- Francis, S. E., Goh, K. L., Hodivala-Dilke, K., Bader, B. L., Stark, M., Davidson, D. and Hynes, R. O. (2002). Central roles of alpha5beta1 integrin and fibronectin in vascular development in mouse embryos and embryoid bodies. *Arterioscler. Thromb. Vasc. Biol.* **22**, 927-933.
- Garmy-Susini, B., Jin, H., Zhu, Y., Sung, R.-J., Hwang, R. and Varner, J. (2005). Integrin alpha4beta1-VCAM-1-mediated adhesion between endothelial and mural cells is required for blood vessel maturation. *J. Clin. Invest.* **115**, 1542-1551.
- George, E. L., Georges-Labouesse, E. N., Patel-King, R. S., Rayburn, H. and Hynes, R. O. (1993). Defects in mesoderm, neural tube and vascular development in mouse embryos lacking fibronectin. *Development* **119**, 1079-1091.
- George, E. L., Baldwin, H. S. and Hynes, R. O. (1997). Fibronectins are essential for heart and blood vessel morphogenesis but are dispensable for initial specification of precursor cells. *Blood* **90**, 3073-3081.
- Grazioli, A., Alves, C. S., Konstantopoulos, K. and Yang, J. T. (2006). Defective blood vessel development and pericyte/pvSMC distribution in alpha 4 integrin-deficient mouse embryos. *Dev. Biol.* **293**, 165-177.
- Hagel, M., George, E. L., Kim, A., Tamimi, R., Opitz, S. L., Turner, C. E., Imamoto, A. and Thomas, S. M. (2002). The adaptor protein paxillin is essential for normal development in the mouse and is a critical transducer of fibronectin signaling. *Mol. Cell. Biol.* **22**, 901-915.
- Hakim, Z. S., DiMichele, L. A., Doherty, J. T., Homeister, J. W., Beggs, H. E., Reichardt, L. F., Schwartz, R. J., Brackhan, J., Smithies, O., Mack, C. P. et al. (2007). Conditional deletion of focal adhesion kinase leads to defects in ventricular septation and outflow tract alignment. *Mol. Cell. Biol.* **27**, 5352-5364.
- Hedin, U. and Thyberg, J. (1987). Plasma fibronectin promotes modulation of arterial smooth-muscle cells from contractile to synthetic phenotype. *Differentiation* **33**, 239-246.
- High, F. A., Zhang, M., Proweller, A., Tu, L., Parmacek, M. S., Pear, W. S. and Epstein, J. A. (2007). An essential role for Notch in neural crest during cardiovascular development and smooth muscle differentiation. *J. Clin. Invest.* **117**, 353-363.
- Holtwick, R., Gotthardt, M., Skryabin, B., Steinmetz, M., Potthast, R., Zetsche, B., Hammer, R. E., Herz, J. and Kuhn, M. (2002). Smooth muscle-selective deletion of guanylyl cyclase-A prevents the acute but not chronic effects of ANP on blood pressure. *Proc. Natl. Acad. Sci. USA* **99**, 7142-7147.
- Horiguchi, M., Ota, M. and Rifkin, D. B. (2012). Matrix control of transforming growth factor-beta function. *J. Biochem.* **152**, 321-329.
- Huo, Y., Guo, X. and Kassab, G. S. (2008). The flow field along the entire length of mouse aorta and primary branches. *Ann. Biomed. Eng.* **36**, 685-699.
- Hynes, R. O. (2007). Cell-matrix adhesion in vascular development. *J. Thromb. Haemost.* **5** Suppl. 1, 32-40.
- Hynes, R. O. (2009). The extracellular matrix: not just pretty fibrils. *Science* **326**, 1216-1219.
- Ito, Y., Yeo, J. Y., Chytil, A., Han, J., Bringas, P., Jr, Nakajima, A., Shuler, C. F., Moses, H. L. and Chai, Y. (2003). Conditional inactivation of Tgfb2 in cranial neural crest causes cleft palate and calvaria defects. *Development* **130**, 5269-5280.
- Jiang, X., Rowitch, D. H., Soriano, P., McMahon, A. P. and Sucov, H. M. (2000). Fate of the mammalian cardiac neural crest. *Development* **127**, 1607-1616.
- Keyte, A. and Hutson, M. R. (2012). The neural crest in cardiac congenital anomalies. *Differentiation* **84**, 25-40.
- Kirby, M. L. and Waldo, K. L. (1995). Neural crest and cardiovascular patterning. *Circ. Res.* **77**, 211-215.
- Kirby, M. L., Gale, T. F. and Stewart, D. E. (1983). Neural crest cells contribute to normal aorticopulmonary septation. *Science* **220**, 1059-1061.
- Lacy-Hulbert, A., Smith, A. M., Tissire, H., Barry, M., Crowley, D., Bronson, R. T., Roes, J. T., Savill, J. S. and Hynes, R. O. (2007). Ulcerative colitis and autoimmunity induced by loss of myeloid alphaV integrins. *Proc. Natl. Acad. Sci. USA* **104**, 15823-15828.
- Li, J., Zhu, X., Chen, M., Cheng, L., Zhou, D., Lu, M. M., Du, K., Epstein, J. A. and Parmacek, M. S. (2005). Myocardin-related transcription factor B is required in cardiac neural crest for smooth muscle differentiation and cardiovascular development. *Proc. Natl. Acad. Sci. USA* **102**, 8916-8921.
- Liaw, L., Skinner, M. P., Raines, E. W., Ross, R., Cheresch, D. A., Schwartz, S. M. and Giachelli, C. M. (1995). The adhesive and migratory effects of osteopontin are mediated via distinct cell surface integrins. Role of alpha v beta 3 in smooth muscle cell migration to osteopontin in vitro. *J. Clin. Invest.* **95**, 713-724.
- Lin, F. and Yang, X. (2010). TGF-beta signaling in aortic aneurysm: another round of controversy. *J. Genet. Genomics* **37**, 583-591.
- Ludbrook, S. B., Barry, S. T., Delves, C. J. and Horgan, C. M. T. (2003). The integrin alphavbeta3 is a receptor for the latency-associated peptides of transforming growth factors beta1 and beta3. *Biochem. J.* **369**, 311-318.
- Meng, H., Wang, Z., Hoi, Y., Gao, L., Metaxa, E., Swartz, D. D. and Kolega, J. (2007). Complex hemodynamics at the apex of an arterial bifurcation induces vascular remodeling resembling cerebral aneurysm initiation. *Stroke* **38**, 1924-1931.

- Mikawa, T. and Gourdie, R. G. (1996). Pericardial mesoderm generates a population of coronary smooth muscle cells migrating into the heart along with ingrowth of the epicardial organ. *Dev. Biol.* **174**, 221-232.
- Mittal, A., Pulina, M., Hou, S.-Y. and Astrof, S. (2010). Fibronectin and integrin alpha 5 play essential roles in the development of the cardiac neural crest. *Mech. Dev.* **127**, 472-484.
- Mittal, A., Pulina, M., Hou, S.-Y. and Astrof, S. (2013). Fibronectin and integrin alpha 5 play requisite roles in cardiac morphogenesis. *Dev. Biol.* **381**, 73-82.
- Moiseeva, E. P. (2001). Adhesion receptors of vascular smooth muscle cells and their functions. *Cardiovasc. Res.* **52**, 372-386.
- Molin, D. G. M., Poelmann, R. E., DeRuiter, M. C., Azhar, M., Doetschman, T. and Gittenberger-de Groot, A. C. (2004). Transforming growth factor beta-SMAD2 signaling regulates aortic arch innervation and development. *Circ. Res.* **95**, 1109-1117.
- Moustakas, A. and Heldin, C.-H. (2005). Non-Smad TGF-beta signals. *J. Cell Sci.* **118**, 3573-3584.
- Munger, J. S., Harpel, J. G., Giancotti, F. G. and Rifkin, D. B. (1998). Interactions between growth factors and integrins: latent forms of transforming growth factor-beta are ligands for the integrin alphavbeta1. *Mol. Biol. Cell* **9**, 2627-2638.
- Munger, J. S., Huang, X., Kawakatsu, H., Griffiths, M. J. D., Dalton, S. L., Wu, J., Pittet, J.-F., Kaminski, N., Garat, C., Matthay, M. A. et al. (1999). A mechanism for regulating pulmonary inflammation and fibrosis: the integrin $\alpha v \beta 6$ binds and activates latent TGF $\beta 1$. *Cell* **96**, 319-328.
- Murphy, P. A. and Hynes, R. O. (2014). Alternative splicing of endothelial fibronectin is induced by disturbed hemodynamics and protects against hemorrhage of the vessel wall. *Arterioscler. Thromb. Vasc. Biol.* **34**, 2042-2050.
- Muzumdar, M. D., Tasic, B., Miyamichi, K., Li, L. and Luo, L. (2007). A global double-fluorescent Cre reporter mouse. *Genesis* **45**, 593-605.
- Neubauer, K., Lindhorst, A., Tron, K., Ramadori, G. and Saile, B. (2008). Decrease of PECAM-1-gene-expression induced by proinflammatory cytokines IFN-gamma and IFN-alpha is reversed by TGF-beta in sinusoidal endothelial cells and hepatic mononuclear phagocytes. *BMC Physiol.* **8**, 9.
- Panda, D., Kundu, G. C., Lee, B. I., Peri, A., Fohl, D., Chackalaparampil, I., Mukherjee, B. B., Li, X. D., Mukherjee, D. C., Seides, S. et al. (1997). Potential roles of osteopontin and alphaVbeta3 integrin in the development of coronary artery restenosis after angioplasty. *Proc. Natl. Acad. Sci. USA* **94**, 9308-9313.
- Papangelis, I. and Scambler, P. (2013). The 22q11 deletion: DiGeorge and velocardiofacial syndromes and the role of TBX1. *Wiley Interdiscip. Rev. Dev. Biol.* **2**, 393-403.
- Pera, J., Korostynski, M., Krzyszkowski, T., Czopek, J., Slowik, A., Dziedzic, T., Piechota, M., Stachura, K., Moskala, M., Przewlocki, R. et al. (2010). Gene expression profiles in human ruptured and unruptured intracranial aneurysms: what is the role of inflammation? *Stroke* **41**, 224-231.
- Piali, L., Hammel, P., Uherek, C., Bachmann, F., Gisler, R. H., Dunon, D. and Imhof, B. A. (1995). CD31/PECAM-1 is a ligand for alpha v beta 3 integrin involved in adhesion of leukocytes to endothelium. *J. Cell Biol.* **130**, 451-460.
- Raines, E. W. (2000). The extracellular matrix can regulate vascular cell migration, proliferation, and survival: relationships to vascular disease. *Int. J. Exp. Pathol.* **81**, 173-182.
- Ray, J. L., Leach, R., Herbert, J.-M. and Benson, M. (2001). Isolation of vascular smooth muscle cells from a single murine aorta. *Methods Cell Sci.* **23**, 185-188.
- Rensen, S. S. M., Doevendans, P. A. F. N. and van Eys, G. J. J. M. (2007). Regulation and characteristics of vascular smooth muscle cell phenotypic diversity. *Neth. Heart J.* **15**, 100-108.
- Savolainen, S. M., Foley, J. F. and Elmore, S. A. (2009). Histology atlas of the developing mouse heart with emphasis on E11.5 to E18.5. *Toxicol. Pathol.* **37**, 395-414.
- Schepke, L., Murphy, E. A., Zarpellon, A., Hofmann, J. J., Merkulova, A., Shields, D. J., Weis, S. M., Byzova, T. V., Ruggeri, Z. M., Iruela-Arispe, M. L. et al. (2012). Notch promotes vascular maturation by inducing integrin-mediated smooth muscle cell adhesion to the endothelial basement membrane. *Blood* **119**, 2149-2158.
- Soriano, P. (1999). Generalized lacZ expression with the ROSA26 Cre reporter strain. *Nat. Genet.* **21**, 70-71.
- Takahashi, S., Leiss, M., Moser, M., Ohashi, T., Kitao, T., Heckmann, D., Pfeifer, A., Kessler, H., Takagi, J., Erickson, H. P. et al. (2007). The RGD motif in fibronectin is essential for development but dispensable for fibril assembly. *J. Cell Biol.* **178**, 167-178.
- ten Dijke, P. and Arthur, H. M. (2007). Extracellular control of TGFbeta signalling in vascular development and disease. *Nat. Rev. Mol. Cell Biol.* **8**, 857-869.
- Todorovic, V., Frenthewey, D., Gutstein, D. E., Chen, Y., Freyer, L., Finnegan, E., Liu, F., Murphy, A., Valenzuela, D., Yancopoulos, G. et al. (2007). Long form of latent TGF-beta binding protein 1 (Ltbp1L) is essential for cardiac outflow tract septation and remodelling. *Development* **134**, 3723-3732.
- Turlo, K. A., Noel, O. D. V., Vora, R., LaRussa, M., Fassler, R., Hall-Glenn, F. and Iruela-Arispe, M. L. (2012). An essential requirement for beta1 integrin in the assembly of extracellular matrix proteins within the vascular wall. *Dev. Biol.* **365**, 23-35.
- Turner, C. J., Badu-Nkansah, K., Crowley, D., van der Flier, A. and Hynes, R. O. (2014). Integrin-alpha5beta1 is not required for mural cell functions during development of blood vessels but is required for lymphatic-blood vessel separation and lymphovenous valve formation. *Dev. Biol.* **392**, 381-392.
- Vallejo-Illarramendi, A., Zang, K. and Reichardt, L. F. (2009). Focal adhesion kinase is required for neural crest cell morphogenesis during mouse cardiovascular development. *J. Clin. Invest.* **119**, 2218-2230.
- van der Flier, A., Badu-Nkansah, K., Whittaker, C. A., Crowley, D., Bronson, R. T., Lacy-Hulbert, A. and Hynes, R. O. (2010). Endothelial alpha5 and alphav integrins cooperate in remodelling of the vasculature during development. *Development* **137**, 2439-2449.
- Veith, C., Marsh, L. M., Wygrecka, M., Rutschmann, K., Seeger, W., Weissmann, N. and Kwapiszewska, G. (2012). Paxillin regulates pulmonary arterial smooth muscle cell function in pulmonary hypertension. *Am. J. Pathol.* **181**, 1621-1633.
- Wagenseil, J. E. and Mecham, R. P. (2009). Vascular extracellular matrix and arterial mechanics. *Physiol. Rev.* **89**, 957-989.
- Waldo, K. L., Hutson, M. R., Ward, C. C., Zdanowicz, M., Stadt, H. A., Kumiski, D., Abu-Issa, R. and Kirby, M. L. (2005). Secondary heart field contributes myocardium and smooth muscle to the arterial pole of the developing heart. *Dev. Biol.* **281**, 78-90.
- Wang, J., Nagy, A., Larsson, J., Dudas, M., Sucov, H. M. and Kaartinen, V. (2006). Defective ALK5 signaling in the neural crest leads to increased postmigratory neural crest cell apoptosis and severe outflow tract defects. *BMC Dev. Biol.* **6**, 51.
- Wang, Y., Dur, O., Patrick, M. J., Tinney, J. P., Tobita, K., Keller, B. B. and Pekkan, K. (2009). Aortic arch morphogenesis and flow modeling in the chick embryo. *Ann. Biomed. Eng.* **37**, 1069-1081.
- Wasteson, P., Johansson, B. R., Jukkola, T., Breuer, S., Akyurek, L. M., Partanen, J. and Lindahl, P. (2008). Developmental origin of smooth muscle cells in the descending aorta in mice. *Development* **135**, 1823-1832.
- Wu, X., Davis, G. E., Meininger, G. A., Wilson, E. and Davis, M. J. (2001). Regulation of the L-type calcium channel by alpha 5beta 1 integrin requires signaling between focal adhesion proteins. *J. Biol. Chem.* **276**, 30285-30292.
- Wurdak, H., Ittner, L. M., Lang, K. S., Leveen, P., Suter, U., Fischer, J. A., Karlsson, S., Born, W. and Sommer, L. (2005). Inactivation of TGFbeta signaling in neural crest stem cells leads to multiple defects reminiscent of DiGeorge syndrome. *Genes Dev.* **19**, 530-535.
- Xie, W.-B., Li, Z., Shi, N., Guo, X., Tang, J., Ju, W., Han, J., Liu, T., Bottinger, E. P., Chai, Y. et al. (2013). Smad2 and myocardin-related transcription factor B cooperatively regulate vascular smooth muscle differentiation from neural crest cells. *Circ. Res.* **113**, e76-e86.
- Yang, J. T. and Hynes, R. O. (1996). Fibronectin receptor functions in embryonic cells deficient in alpha 5 beta 1 integrin can be replaced by alpha V integrins. *Mol. Biol. Cell* **7**, 1737-1748.
- Yang, J. T., Rayburn, H. and Hynes, R. O. (1993). Embryonic mesodermal defects in alpha 5 integrin-deficient mice. *Development* **119**, 1093-1105.
- Yang, Z., Mu, Z., Dabovic, B., Jurukovski, V., Yu, D., Sung, J., Xiong, X. and Munger, J. S. (2007). Absence of integrin-mediated TGFbeta1 activation in vivo recapitulates the phenotype of TGFbeta1-null mice. *J. Cell Biol.* **176**, 787-793.
- Yang, M., Jiang, H. and Li, L. (2010). Sm22alpha transcription occurs at the early onset of the cardiovascular system and the intron 1 is dispensable for its transcription in smooth muscle cells during mouse development. *Int. J. Physiol. Pathophysiol. Pharmacol.* **2**, 12-19.
- Yashiro, K., Shiratori, H. and Hamada, H. (2007). Haemodynamics determined by a genetic programme govern asymmetric development of the aortic arch. *Nature* **450**, 285-288.
- Zhao, J. J., Gjoerup, O. V., Subramanian, R. R., Cheng, Y., Chen, W., Roberts, T. M. and Hahn, W. C. (2003). Human mammary epithelial cell transformation through the activation of phosphatidylinositol 3-kinase. *Cancer Cell* **3**, 483-495.
- Zilberberg, L., Todorovic, V., Dabovic, B., Horiguchi, M., Couroussé, T., Sakai, L. Y. and Rifkin, D. B. (2012). Specificity of latent TGF-beta binding protein (LTBP) incorporation into matrix: role of fibrillins and fibronectin. *J. Cell Physiol.* **227**, 3828-3836.

Supplementary Materials and Methods

Histology and immunofluorescence staining

Freshly isolated embryos were embedded in Tissue-Tek OCT and sectioned (20 μm) on a Cryostat; or fixed in 4% paraformaldehyde (PFA) in PBS at 4°C overnight or in zinc fixative (BD) at room temperature (RT) for 48 hours, followed by embedding and sectioning (5 μm) in paraffin. Selected paraffin sections were stained with hematoxylin and eosin (H&E) using standard protocols.

For immunofluorescence staining, deparaffinized tissue sections were subjected to heat-induced epitope retrieval (2x5 min 800 W microwave) in 10 mM Tris Base, 1 mM EDTA Solution, 0.05% Tween 20, pH 9.0, blocked in PBS containing 0.5% Tween (PBS-T) and 2% goat, donkey or fibronectin-depleted goat serum and incubated overnight at 4°C with primary antibodies diluted in 1:1 PBS:PBS-T. After washes in PBS, tissues were incubated either at RT for 2 hours, or overnight at 4°C, with fluorophore-conjugated secondary antibodies diluted in 1:1 PBS-T. Samples were then washed in PBS, mounted onto coverslips in Fluoromount (Southern Biotech) and imaged using Zeiss LSM 510 or Nikon A1R scanning laser confocal microscopes. All images were processed using Volocity (Perkin Elmer) or Nikon Elements software. For whole-mount stainings, embryonic back skin from PFA-fixed embryos was removed and stained following the methods previously described in Foo et al. (2006). Staining for β -galactosidase (LacZ) activity; whole embryos or organs were dissected, fixed in 0.2% glutaraldehyde, 5mM EGTA, 2 mM MgCl_2 in PBS for 15 min at RT and stained following methods previously described in Nagy (2003).

vSMC isolation and culture

The aorta was dissected and all extra tissue and adventitia removed. The aorta was then cut into 2 mm pieces and placed in collagenase type II for 4 hrs at 37°C, 5% CO_2 . Digestion was stopped by the addition of fresh culture medium (DMEM containing 10% fetal calf serum, 2 mM L-glutamine), centrifugation, and resuspension in fresh medium. The cells were then transferred to a single well of a 48-well plate and left undisturbed for 5 days at 37°C, 5% CO_2 .

Immunofluorescence staining of cells

For immunofluorescence experiments, cells were plated onto glass coverslips coated with Matrigel (20 $\mu\text{g}/\text{ml}$), and fixed with 4% PFA or ice-cold methanol (for integrin α_v staining). The cells were then permeabilised with 0.1% Triton X-100, blocked for 1 h at room temperature in PBS containing 2% BSA, and incubated with primary antibodies diluted in blocking solution overnight at 4°C. After washing, cells were incubated with fluorophore-conjugated secondary antibodies at room temperature for 1 h, washed, and mounted onto glass slides in Fluoromount.

Antibodies

Rat anti-mouse PECAM-1 MEC13.3, rat anti-mouse Integrin- α_5 (BD Pharmingen), mouse anti-human αSMA Clone1A4-Cy3, mouse anti-Vinculin, mouse anti-Vimentin (Sigma), goat anti-GFP, rabbit anti-Fibulin 5, rabbit anti-

Elastin, rabbit anti-Fibronectin, rabbit anti-Collagen IV, rabbit anti-Fibrillin 1, rabbit anti-Paxillin, rabbit anti-Myh11, rabbit anti-SM22 α (Abcam), Rabbit anti-FAK, rabbit anti-pFAK (pTyr397), rabbit anti-p130Cas (Y165), rabbit anti-pCRKL (Y207), rabbit anti-pSMAD2, rabbit anti-SMAD2, rabbit anti-SMAD1 (Cell Signaling), Rabbit anti-LTBP-1 (Abgent), Goat anti-Smoothelin, rabbit anti-LTBP-3 (Santa Cruz), mouse anti-GAPDH, Rabbit anti-Itg α v, rabbit anti-Itg α 5, rabbit anti-pSMAD1/5/8 (Millipore).

Secondary antibodies were Alexa488, Alexa594, and Alexa647 conjugated antibodies (Invitrogen).

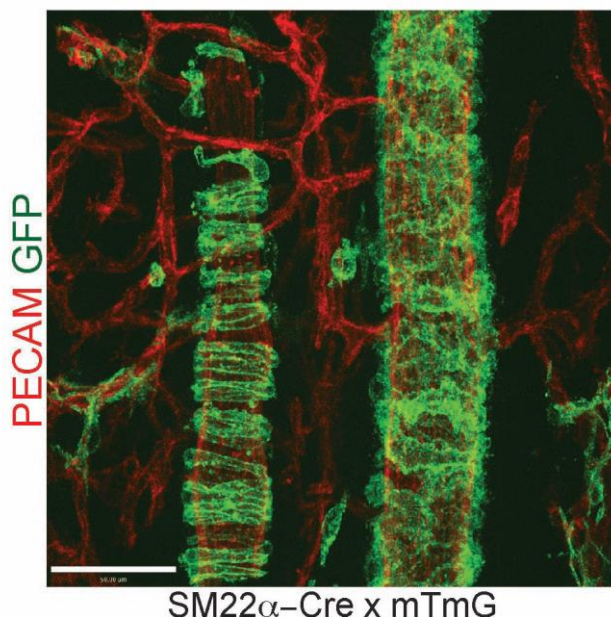
Immunoblotting

Novex Tris-glycine precast gels (Invitrogen) were used and wet-transferred to nitrocellulose. Blots were blocked and incubated with antibodies in 5% non-fat dried milk, 0.2% NP40, Tris-buffered saline (pH 8). Primary antibodies were integrin α 5 (AB1928), α v (AB1930) and GAPDH (MAB374) (all from Millipore), vimentin (Sigma), and rabbit anti-fibronectin (297.1; generated in our laboratory). HRP-conjugated secondary antibodies were from Jackson ImmunoResearch: goat anti-rabbit and sheep anti-mouse IgM and HRP-streptavidin. Blots were developed using Western-Lightning ECL (PerkinElmer).

Real-time RT-PCR

RNA was isolated from cells using the RNAeasy kit (Qiagen) following the manufacturers' guidelines. cDNA synthesis was achieved by mixing 1 μ g of total RNA with 100 pmole random hexamer primers and the Reverse Transcription System kit (Promega). Real-time RT-PCR was carried out using 5 ng of cDNA, 300 nmoles of each primer (see table below) and 12.5 μ l of IQ SYBR green Supermix (Bio-Rad).

Gene	Forward Primer	Reverse Primer
<i>Eln</i>	GGCTTTGGACTTTCTCCATT	CCGGCCACAGGATTTCC
<i>Fn1</i>	CTTTGGCAGTGGTCATTTTCAG	ATTCTCCCTTTCCATTCCCG
<i>Hspg2</i>	TACGCGGTCCATTGAG	AGATCCGTCCGCATTC
<i>Nd1</i>	AACAATAGACACCAGTGCTCC	TCCCTTCACCTTGCCATTG
<i>Fbn1</i>	AATGAAGGCTATGAGGTGGC	TCTGTAGACTATACCCAGGCG
<i>Col1a1</i>	CATAAAGGGTCATCGTGGCT	TTGAGTCCGTCTTTGCCAG
<i>Fbln4</i>	AGCTACACGGAATGCACAG	AGGCAGACACAAATAACCCC
<i>Fga</i>	GAGAAAGCGCAACAGATTCAAG	TTATCTCACGGTTTACAGCCC
<i>Lamb1</i>	GGCAAAGTCAAAGTCTCG	CTGGAGGTGTTCCACAGGTC
<i>Fbln5</i>	ATGTCGCTATGGTTACTGCC	GGTCTGAACACAGGGATTCTC
<i>Cola4a1</i>	AGACCATTTCAGATTCCGCAG	CGCTTCTAAACTCTTCCAGACAG
<i>Vtn</i>	CTACCGAGTCAACCTTAGAACC	GAAAGAGATGAGGCTCCTGAAG
<i>tgfb1</i>	CCTGAGTGGCTGTCTTTTGA	CGTGGAGTTTGTATCTTTGCTG
<i>Itga1</i>	CCAACTCCAGTACATACCTGC	CTCCCACTTTATAGCTCCATT
<i>Itga2</i>	CGATACACATAACCCTCAGCTC	CTGCCTATGATAACCCCTGTC
<i>Itga4</i>	ATAAAGGCAAAGAGGTCCAG	CGTCAGAAGTCCATTAGAGAAG
<i>Itga5</i>	TGGAAGTCAGAAAGAGAATGGAG	GGTTCTTAGAATCCGAGACTGG
<i>Itga6</i>	GAGAGGCTTACTTCCGATGC	CCATGTGTTTCTCATCTTTGATCTC
<i>Itga8</i>	CATTGCTGTTTCATCTTGCC	CAGTAAAGACAACCCCAGAGG
<i>Itga9</i>	ATGAAGATGGTTGGGACTGG	ACAAAGATCAAGGACCACAGG
<i>Itga10</i>	CATCCCAACCCTCATCCTTC	AAGCCCCGAAGAGTAAATGG
<i>Itga11</i>	CTATGAGTGACCCAGAGTTGTG	CTGCTTTCTGATGTTTGGAAGG
<i>Itgav</i>	ACAGATGCAGTGTGAGGAAC	AAATGGTGATGGGAGTGAGC
<i>Itgb1</i>	TCCTATTTACAAGAGTGCCGTG	CCCTACTGTGACTAAGATGCTG
<i>Itgb2</i>	CAAACACAACGTGGCTTACAG	ACAATTCTTAGGGCTCTGCG
<i>Itgb3</i>	CAGTACTACGAAGACACCAGTG	CCAGATGAGCAGAGTAGCAGG
<i>Itgb4</i>	AGTGGGTAGAGGTGATACAAGG	TTAAGTGCAGAACAAAAGGCTG
<i>Itgb5</i>	TTCAGCTACACAGAAGTCC	GAGTGCCATCCCAATCAGG
<i>Itgb6</i>	AGTACCCAAGAACAAGTCC	CTTCCAGTTCACCTCAGAC
<i>Itgb7</i>	TCACAACCACTGTCAACCC	TCTTTGCCTGACAGACGC
<i>Itgb8</i>	TGAAGAGTGTGCCATGAAGAC	GCTACAACACTAGTCTCCAACAG



Supplementary Figure 1. Confirmation of vascular smooth muscle cell-specific expression of the *SM22 α -Cre* recombinase.

(A) *SM22 α -Cre*-mediated activation of the mTmG reporter, in which Cre-mediated excision results in the expression of membrane-bound GFP, in vascular smooth muscles (GFP, green), but not endothelial cells (red, PECAM-1) in the embryonic skin at E17.5. Scale bar: 50 μ m.

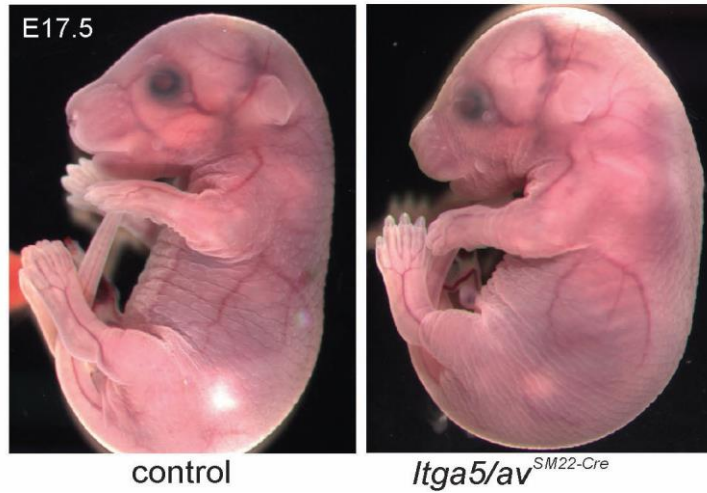
Survival Numbers

	control	<i>Itga5</i> ^{SM22-cre}	<i>Itgav</i> ^{SM22-cre}	<i>Itga5/av</i> ^{SM22-cre}
E12.5	9	9 (100%)	10 (100%)	8 (89%)
E13.5	17	15 (88%)	22 (100%)	13 (76%)
E14.5	7	9 (100%)	9 (100%)	9 (100%)
E15.5	5	5 (100%)	5 (100%)	5 (100%)
E17.5	23	24 (100%)	26 (100%)	12 (52%)
P21	59	29 (49%)	23 (39%)	0 (0%)

Supplementary Figure 2. Survival numbers of *Itga5*^{SM22-Cre}, *Itgav*^{SM22-Cre} and *Itga5/av*^{SM22-Cre} mutant mice.

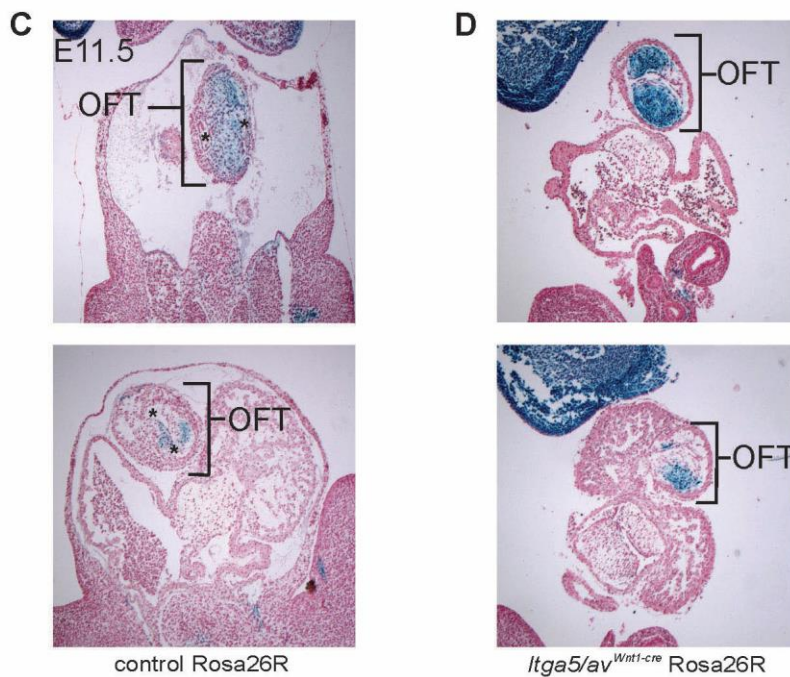
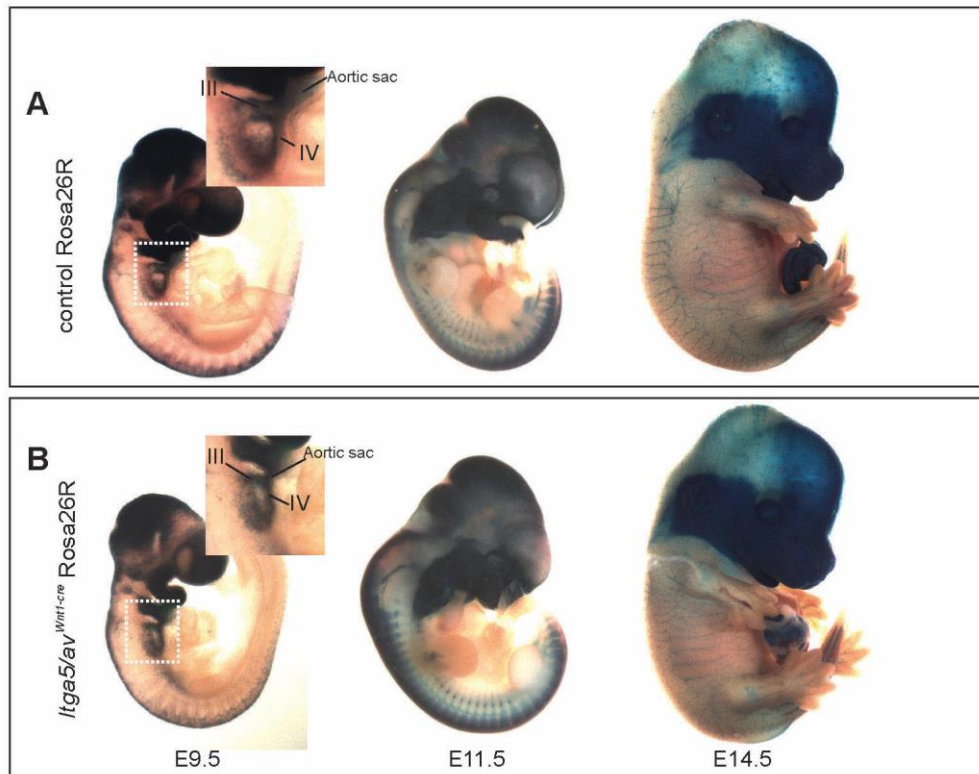
Table showing the number of live mutant mice, collected at the indicated

developmental times. Percentages of live mice, as compared to controls (*Itga5^{flox/-}; Itgav^{flox/-}*), are shown in parentheses.



Supplementary Figure 3. Normal blood vessel morphology in vasculature of the skin.

Freshly isolated E17.5 control and *Itga5/av^{SM22-Cre}* embryos. Note absence of obvious vascular defects and slight growth retardation.



Supplementary Figure 4. Normal neural crest distribution in *Itga5/av^{Wnt1-Cre}* mutant mice.

Whole-mount Xgal-stained (blue) control (A) and *Itga5/av^{Wnt1-Cre}* mutants (B) containing the Rosa26lacZ Cre reporter (Rosa26R) at indicated ages. Note *Wnt1*-positive neural crest cells in the aortic sac/outflow tract and III and IV pharyngeal arch arteries in both control and mutant embryos (enlarged images)

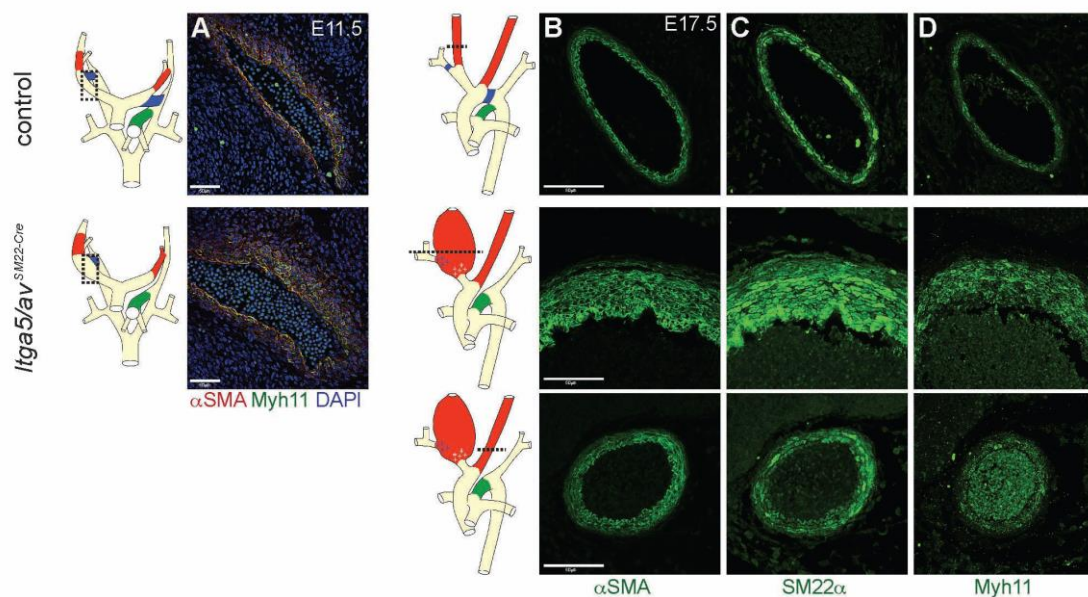
in insets). Sequential frontal sections through the outflow tract (OFT) of Rosa26R Cre reporter stained with Xgal (blue) in control (C) and *Itga5/av*^{Wnt1-Cre} mutant (D) at E11.5. Note that the cushions of the outflow tract (OFT) are already starting to septate the vessel into the pulmonary artery and aorta in control (indicated with an asterisks C).

Survival Numbers

	control	<i>Itga5</i> ^{Wnt1-cre}	<i>Itgav</i> ^{Wnt1-cre}	<i>Itga5/av</i> ^{Wnt1-cre}
E10.5	3	3 (100%)	1 (33%)	5 (100%)
E11.5	8	9 (100%)	16 (100%)	14 (100%)
E15.5	6	5 (83%)	6 (100%)	5 (83%)
E17.5	24	24 (100%)	16 (67%)	12 (50%)
P21	22	0 (0%)	2 (9%)	0 (0%)

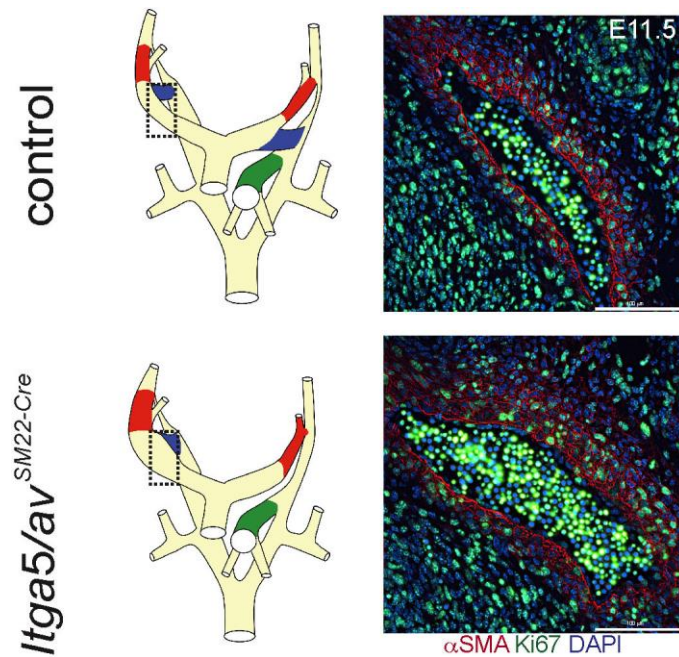
Supplementary Figure 5. Survival numbers of *Itga5*^{Wnt1-Cre}, *Itgav*^{Wnt1-Cre} and *Itga5/av*^{Wnt1-Cre} mutant mice.

Table showing the number of live neural crest-specific mutants, collected at indicated developmental times. Percentage of live embryos or mice, as compared to controls shown in parentheses.



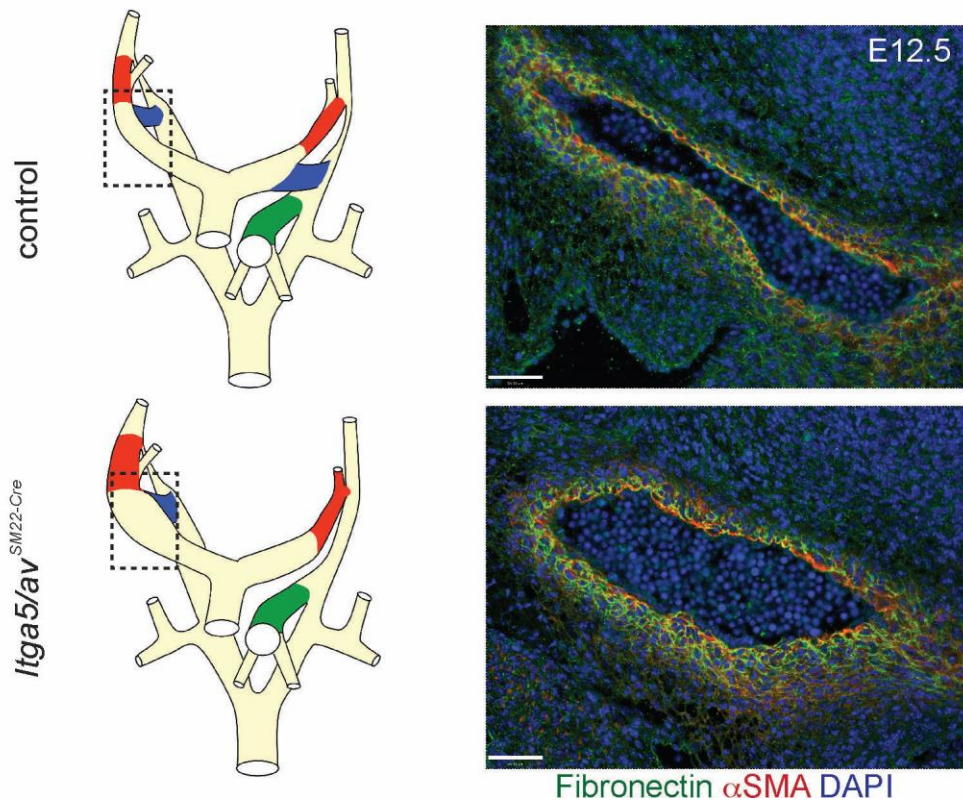
Supplementary Figure 6. Normal vSMC differentiation in *Itga5/av^{SM22-Cre}* mice.

(A) Frontal section through the brachiocephalic artery showing expression of α SMA (red) and Myh11 (green) in control and *Itga5/av^{SM22-Cre}* embryos at E11.5. (B-D) Immunofluorescence stained transverse sections from E17.5 embryos confirming both control and *Itga5/av^{SM22-Cre}* mice maintain expression of α SMA (B), SM α 22 (C), and Myh11 (D) in their neural-crest-derived vSMCs. Scale bars: 50 μ m (A-D).



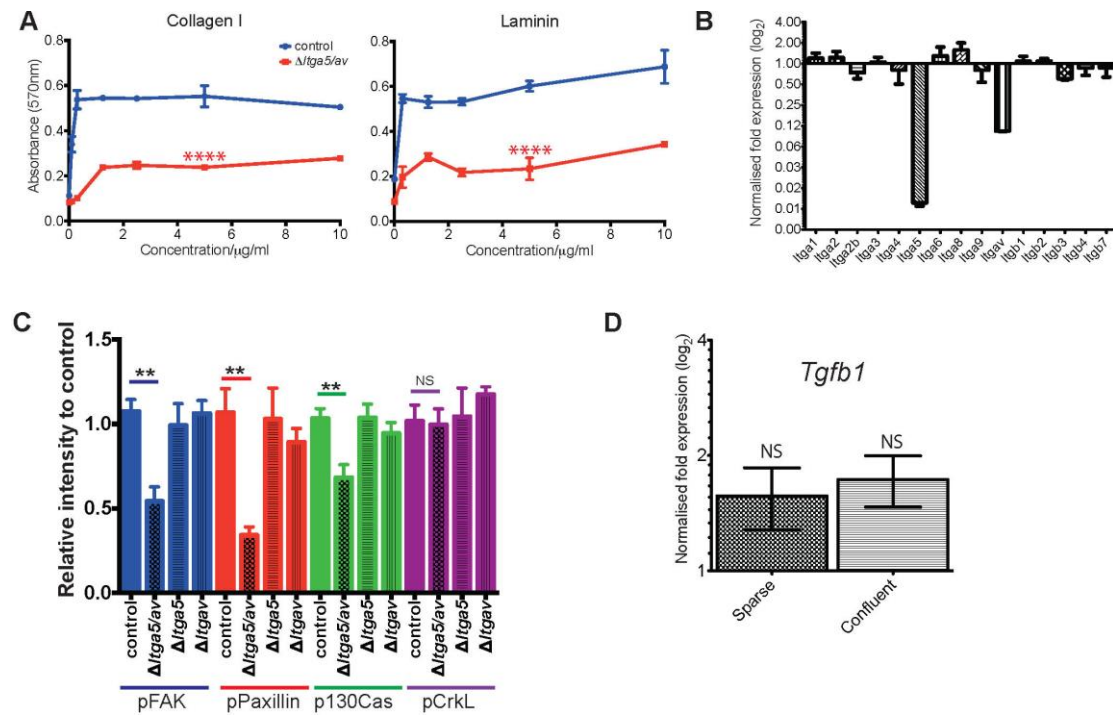
Supplementary Figure 7. No obvious proliferation defects within the vessel wall of *Itga5/av^{SM22-Cre}* mice.

Frontal section through the brachiocephalic artery showing expression of α SMA (red) and Ki67 (green) in control and *Itga5/av^{SM22-Cre}* embryos at E11.5. Scale bars: 100 μ m.



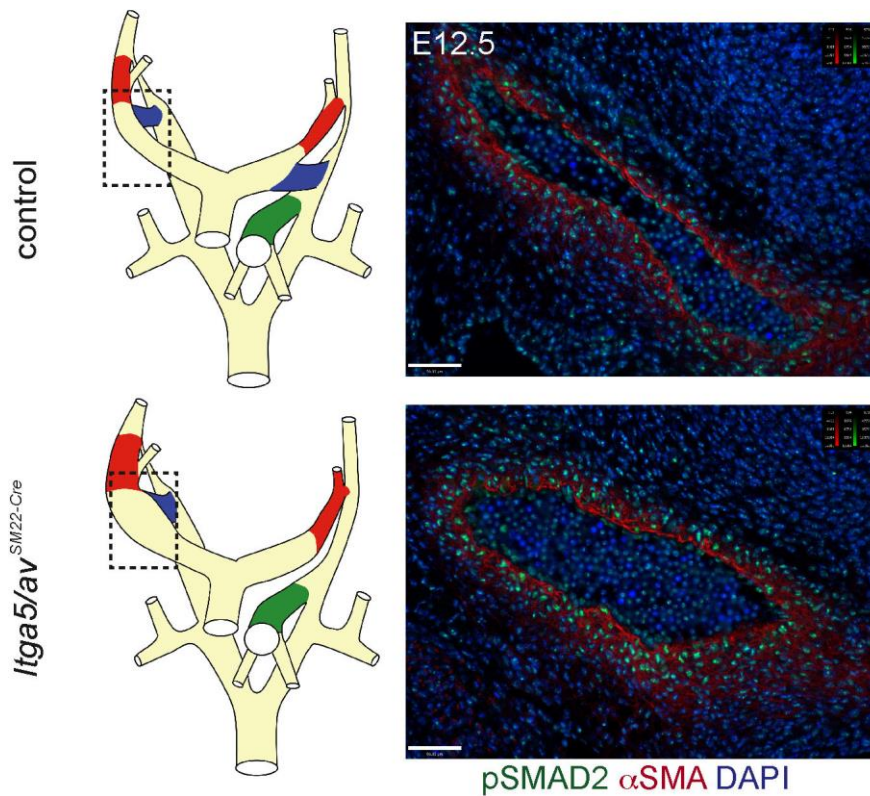
Supplementary Figure 8. No obvious defects in the assembly of fibronectin within the vessel wall of *Itga5/av^{SM22-Cre}* mice.

Frontal sections through the right carotid artery of an E12.5 control and *Itga5/av^{SM22-Cre}* embryo immunostained with anti-fibronectin antibody (green). Note the lack of any obvious defects in the assembly of fibronectin in the *Itga5/av^{SM22-Cre}* embryo, notwithstanding dilation of the vessel. Scale bars: 50 μ m.



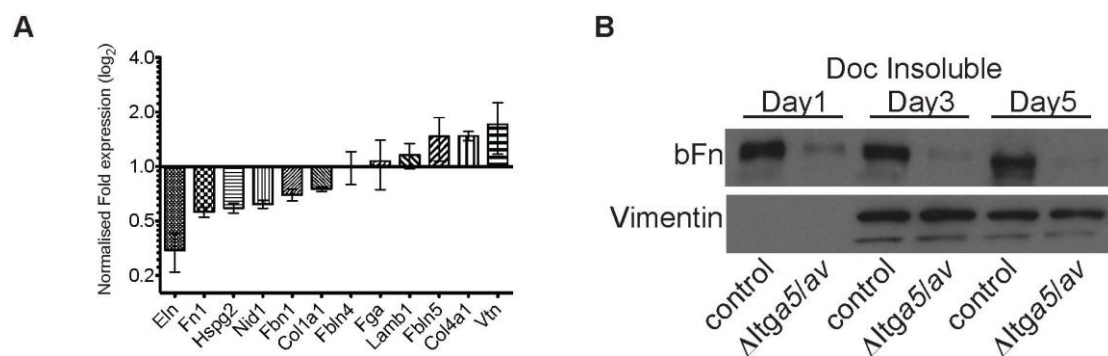
Supplementary Figure 9. Characterisation of $\Delta Itga5/av$ vSMCs.

(A) Cell adhesion assay showing that $\Delta Itga5/av$ vSMCs have decreased adherence to collagen I and laminin. (B) Expression of integrins in $\Delta Itga5/av$ vSMCs as compared to control cells. (C) Quantification of western blots from Fig. 6F. (D) Real-time RT-PCR showing somewhat elevated *Tgfb1* expression in $\Delta Itga5/av$ cells plated on Matrigel at both sparse or confluent conditions normalised to control cells.



Supplementary Figure 10. TGF- β signalling in E12.5 embryos.

Frontal section through the brachiocephalic/carotid artery showing expression of α SMA (red) and pSMAD2 (green), in control and *Itga5/av*^{SM22-Cre} embryos at E12.5. Note the increased expression of pSMAD2 in vessel wall of the *Itga5/av*^{SM22-Cre} embryo. Scale bars: 50 μ m.



Supplementary Figure 11. Expression and assembly of ECM proteins by Δ *Itga5/av* vSMCs.

(A) ECM expression by Δ *Itga5/av* vSMCs normalised to control cells. (B) DOC-insolubility assay showing that Δ *Itga5/av* vSMCs cannot incorporate exogenous biotin-labelled fibronectin into the matrix over 5 days in culture.

Foo, S. S., Turner, C. J., Adams, S., Compagni, A., Aubyn, D., Kogata, N., Lindblom, P., Shani, M., Zicha, D. and Adams, R. H. (2006) 'Ephrin-B2 controls cell motility and adhesion during blood-vessel-wall assembly', *Cell* 124(1): 161-73.
Nagy, A. (2003) *Manipulating the mouse embryo : a laboratory manual*, Cold Spring Harbor, N.Y.: Cold Spring Harbor Laboratory Press.